Karsologie

Jiří Faimon

rozsah 2/0

3 kredity

Krasové speleotémy - archiv informací

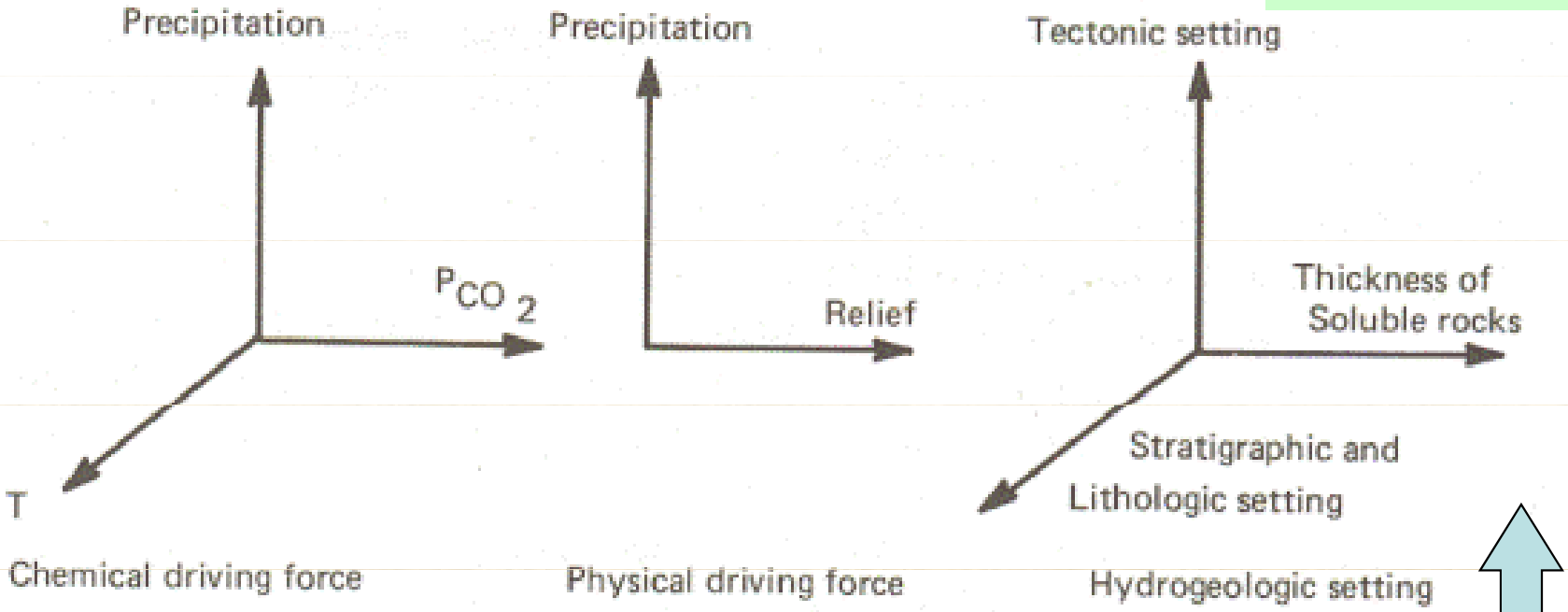

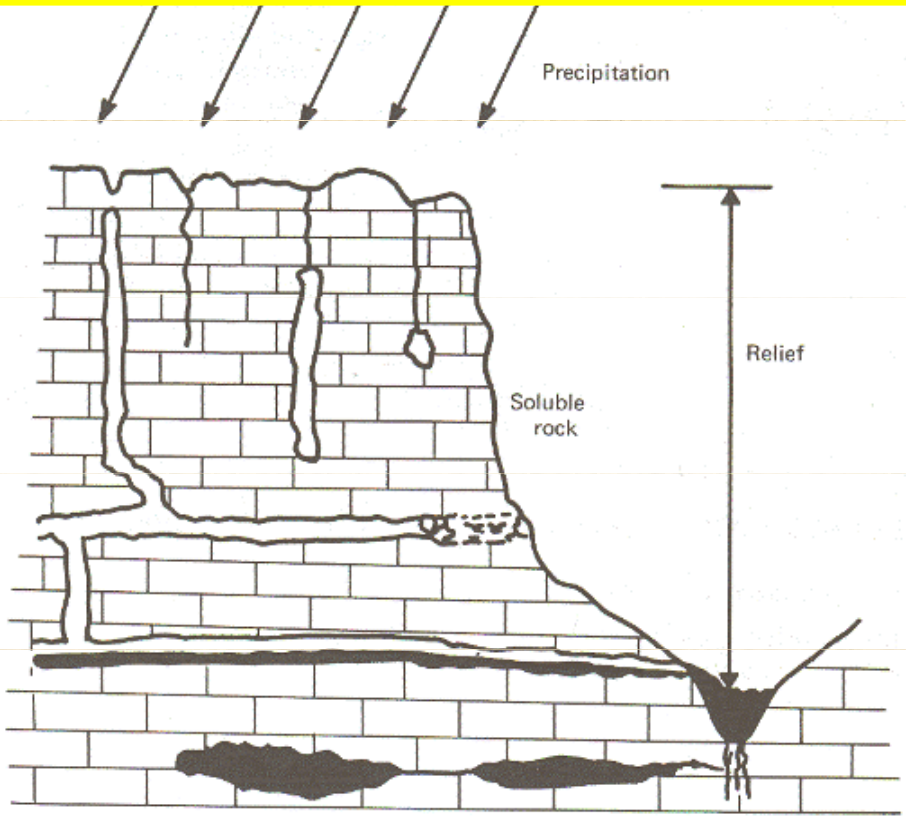

krasový vývoj
7 proměnných

Tři proměnné výrazně řízeny klimatem:
(1) srážky, (2) teplota, (3) produkce CO_2
Systematické variace v různě dlouhých časových úsecích (sezónní a jiné cykly).
V centru našeho zájmu - **klimatické změny** v posledních 10 000 až 100 000 letech.

Kras - archiv informací

Vývoj krajiny je o několik řádů pomalejší, než může člověk přímo sledovat:

- mladé krajiny, ~ 20 ka, vývoj po ústupu zalednění
- krajiny nesrovnatelně starší, > 40Ma, formované již od Terciéru

Dnešní klima je odlišné od klimatu v geologické minulosti!

Teplota, srážky a produkce CO_2 variovali v širokém rozmezí během vývoje krajiny.

V krasu a jeskyních jsou zaznamenány **informace o historii krajiny**

- jeskynní pasáže samotné – záznam o průtocích vody (paleodischarges)
- sekvence jeskyní ve vertikáním profilu krasu (patra) – informace o změnách regionální erozní báze
- velký balík paleoinformací: ve speleotémách a klastických sedimentech.

Problémem - rozluštění záznamu

Datování v krasu

Mnoho **metod pro datování** klastických sedimentů a sintrů

Nedostatky metod:

- nepokrývají celou časovou škálu od současnosti do středního Pliocénu
- poskytují věk výplní (uloženin) spíš než věk jeskynní samotných (vztahy mezi jeskyní a výplněmi pak musí být určeny z vnějších vztahů)

Datovací techniky:
rozsah využití

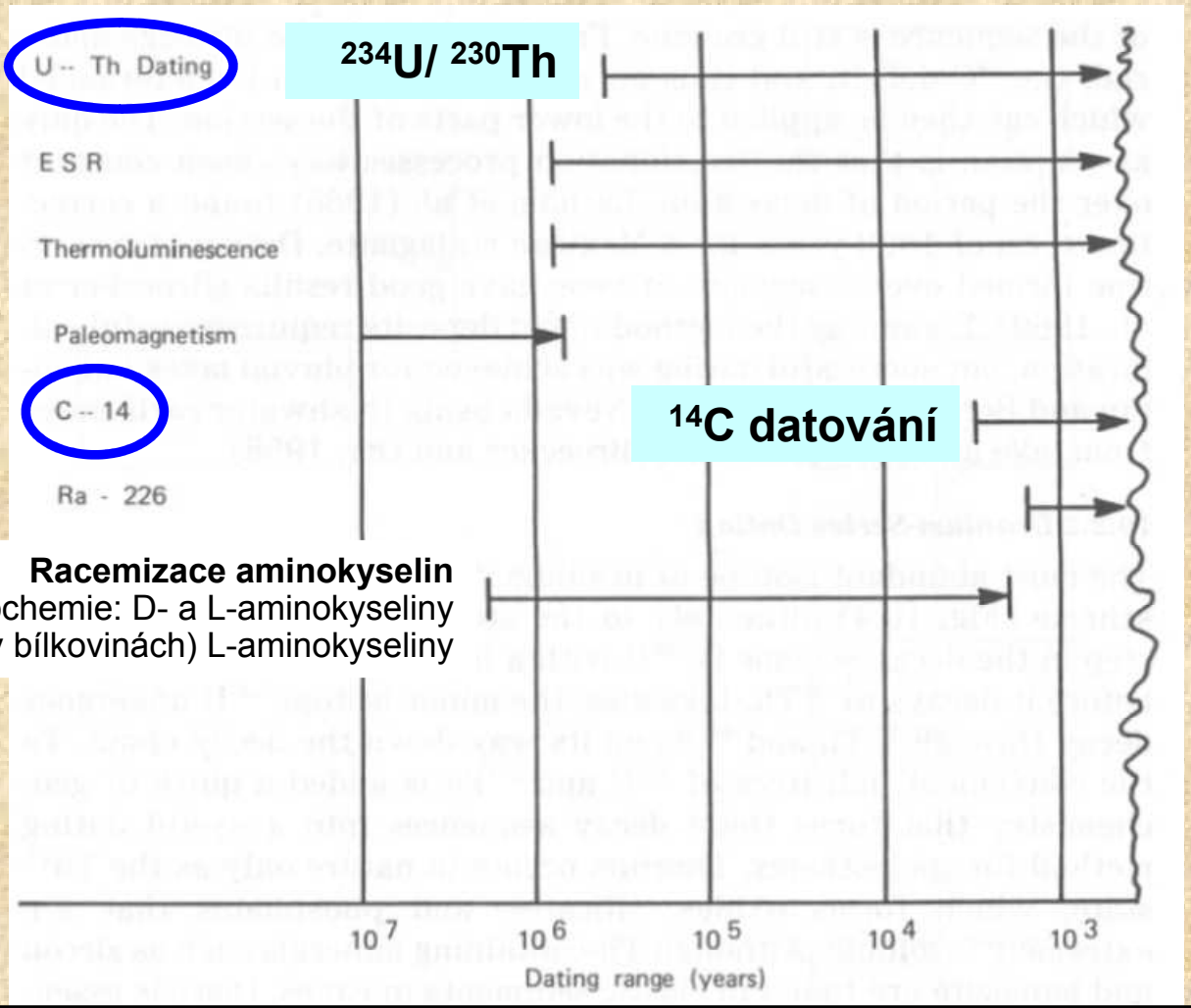

Racemizace aminokyselin
Stereochemie: D- a L-aminokyseliny
V živé hmotě (v bílkovinách) L-aminokyseliny

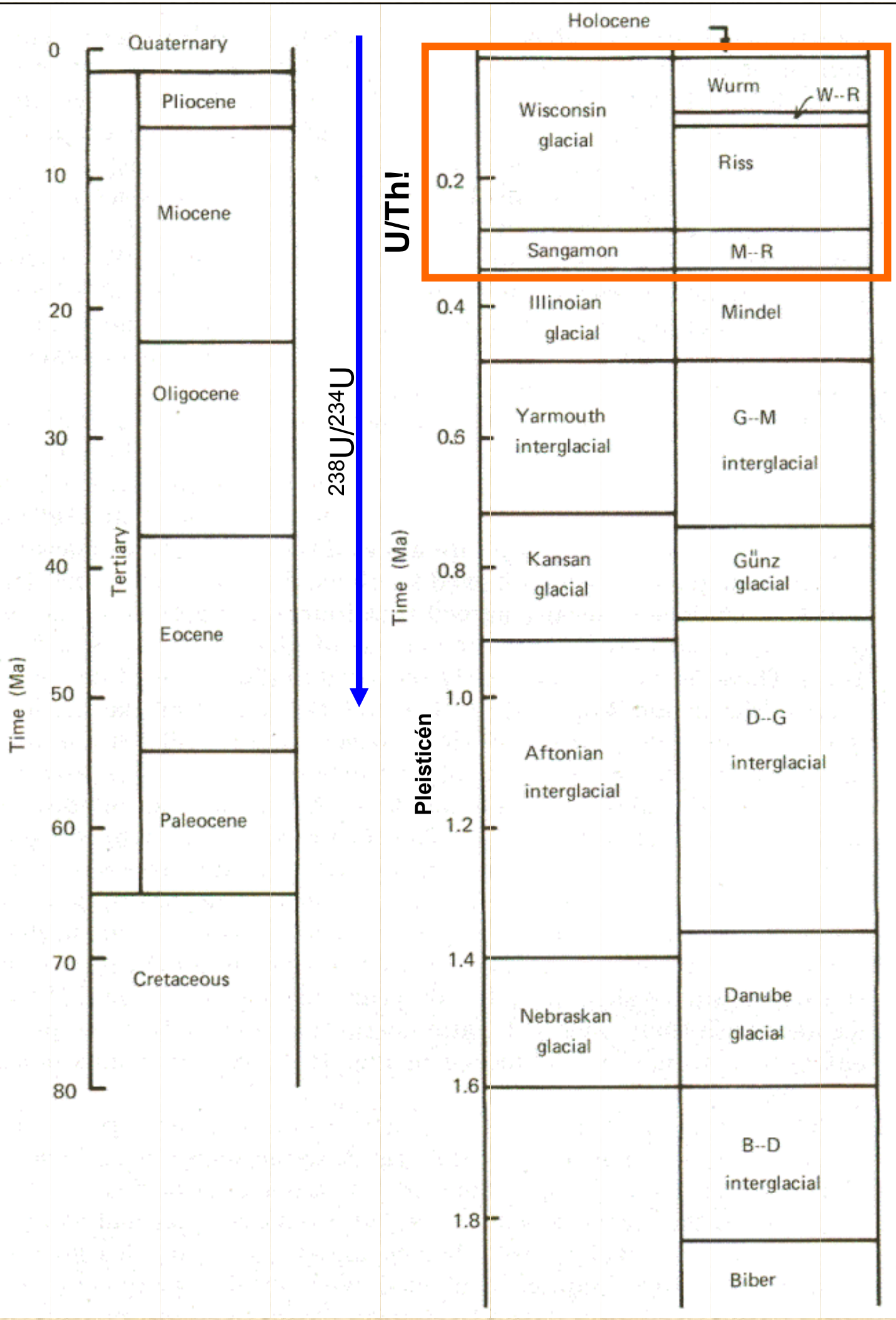
Time (Ma)
0
10
20
30
40
50
60
70
80
Quaternary
Pliocene
Miocene
Oligocene
Eocene
Paleocene
Cretaceous
Tertiary
238U/234U
U/Th!
Holocene
Wurm
W--R
Wisconsin glacial
Riss
Sangamon
M--R
Illinoian glacial
Mindel
Yarmouth interglacial
G--M interglacial
Kansan glacial
Günz glacial
Aftonian interglacial
D--G interglacial
Nebraskan glacial
Danube glacial
B--D interglacial
Biber
Pleistocén
Time (Ma)
0.2
0.4
0.6
0.8
1.0
1.2
1.4
1.6
1.8

Tisíce let B.P.	Alpský syst. a)	Alpský syst. b)	Nordický syst.	Britský syst.	severoamer. syst.
0 - 11	holocén	holocén	Holocén /flandr	holocén/flandr	holocén
11- 120	würm (5./4. led. doba)	würm (5./4. led. doba)	Vistulan (=vislan)	devens	wisconsin
120 - 128	ris-würm (= riss-würm)	ris-würm (=riss-würm)	ém (=eem)	ipswich	sangamon
128 - 365	ris (=riss, 4./3. led. doba)	ris = riss, 4./3. led. doba) + mindel-ris (=mindel-riss)	sál (=saale)	wolston	illinoian (od MIS 8) + preillinoian – pokrač.
365 – 405 / 425			Holstein	hoxne	preillinoian
405/425 – 478		mindel (3./2. led. . doba)	elster	anglian	
478 - 865	mindel-ris (=mindel-riss) + mindel (3./2. led. doba) + *günz-mindel (*resp. mindel-haslach + haslach + haslach-günz)	günz-mindel + günz (2./1. led. doba) + donau-günz + (?) donau (1./0. led. doba)	kromer	kromer (od MIS 19) + beeston	
865 – 1770 (začátek pleistocénu)	günz (2./1. led. doba) + donau-günz + donau (1./0. led. . doba)	?	bavel + menap + vál + eburón		
1770 – 2560 / 2590 (přechod pleistocénu a pliocénu)	(?) biber-donau + biber	?	tegelén + pretegelén (=brügen)	paston + prepaston(=bavent) + bramerton (=ant) + thurne	
>2560/ 2590 (konec pliocénu)	?	?	reuver + brunssum	?	?

Datování pomocí radiogenních izotopů

Rychlost radioaktivního rozpadu (počet přeměněných atomů za čas **t**) je úměrná počtu nerozpadlých atomů ***N***, **λ** je rozpadová konstanta (rok^{-1})

$$-\frac{dN}{dt} = \lambda N$$

Integrace: $N = N_0 e^{-\lambda t}$

Mateřský a dceřiný izotop: ***P - parent, D - daughter***

$$N_P = N_{P_0} e^{-\lambda t}$$

Dceřiný izotop z rozpadu: $N_D^* = N_{P0} - N_P \rightarrow N_{P0} = N_D^* + N_P$

$$N_D^* = N_P (e^{\lambda t} - 1)$$

Měřený $N_D = N_D^* + N_{D0}$

$$N_D = N_{D^0} + N_P (e^{\lambda t} - 1)$$

Poločas rozpadu, $t_{1/2}$, je definován jako doba (např. v Ma), za kterou dojde k rozpadu poloviny mateřských atomů na atomy dceřiné

$$t_{1/2} = \frac{\ln 2}{\lambda} = \frac{0{,}693}{\lambda}$$

TABLE 7.1. Half-lives and decay constants of long-lived U and Th daughters

Nuclide	Half-life, yrs	Decay constant, yr^{-1}	Parent
^{234}U	246,000	2.794×10^{-6}	^{238}U
^{231}Pa	32,480	2.134×10^{-5}	^{235}U
^{230}Th	75,200	9.217×10^{-6}	^{238}U
^{226}Ra	1,622	4.272×10^{-4}	^{238}U
^{220}Ra	6.7	1.06×10^{-1}	^{232}Th
^{210}Pb	22.26	3.11×10^{-2}	^{238}U

Some radioactive decay schemes of interest in sedimentary geology

Radioactive parent isotope	Radiogenic daughter isotope	Decay mechanism	Decay constant (λ)	Half-life[a] ($T_{1/2}$), billion years
^{87}Rb	^{87}Sr	Beta	1.42×10^{-11}	48.8
^{147}Sm	^{143}Nd	Alpha	6.54×10^{-12}	106
^{238}U[b]	^{234}U**, ^{230}Th**, ^{206}Pb	Alpha and beta	1.551×10^{-10}	4.468
^{235}U[b]	^{231}Pa**, ^{207}Pb	Alpha and beta	9.8485×10^{-10}	0.704
^{232}Th[b]	^{208}Pb	Alpha and beta	4.9475×10^{-11}	14.010
^{40}K	^{40}Ar	Electron capture	0.581×10^{-10}	11.93[c]
^{40}K	^{40}Ca	Beta	4.962×10^{-10}	1.397[c]
^{187}Re	^{187}Os	Beta	1.64×10^{-11}	42.3
^{138}La	^{138}Ce	Beta branched decay	2.24×10^{-12}	310
^{176}Lu	^{176}Hf	Beta	1.94×10^{-11}	35.7
^{14}C	^{14}N	Beta	1.75×10^{-4}	5730 years
^{137}Cs	^{137}Ba	Beta	2.29×10^{-2}	30.3 years

Data from compilations by Faure (1986), Blum (1995), Dickin (1995), and Brownlow (1997).

Rozpadové řady

$^{235}U \rightarrow {}^{207}Pb$

Izotop	Poločas přeměny	Přeměna	
^{235}U	$7{,}04 \cdot 10^{8}$ r	α	
^{231}Th	25,52 h	β^-	
^{231}Pa	$3{,}276 \cdot 10^{4}$ r	α	
^{227}Ac	21,772 r	β^-	α (1,38 %)
^{227}Th	18,68 d	α	
^{223}Fr	22,00 min	β^-	
^{223}Ra	11,43 d	α	
^{219}Rn	3,96 s	α	
^{215}Po	$1{,}781 \cdot 10^{-3}$ s	α	
^{211}Pb	36,1 min	β^-	
^{211}Bi	2,14 min	β^-	α (99,72 %)
^{211}Po	0,516 s	α	
^{207}Tl	4,77 min	β^-	
^{207}Pb	*stabilní*		

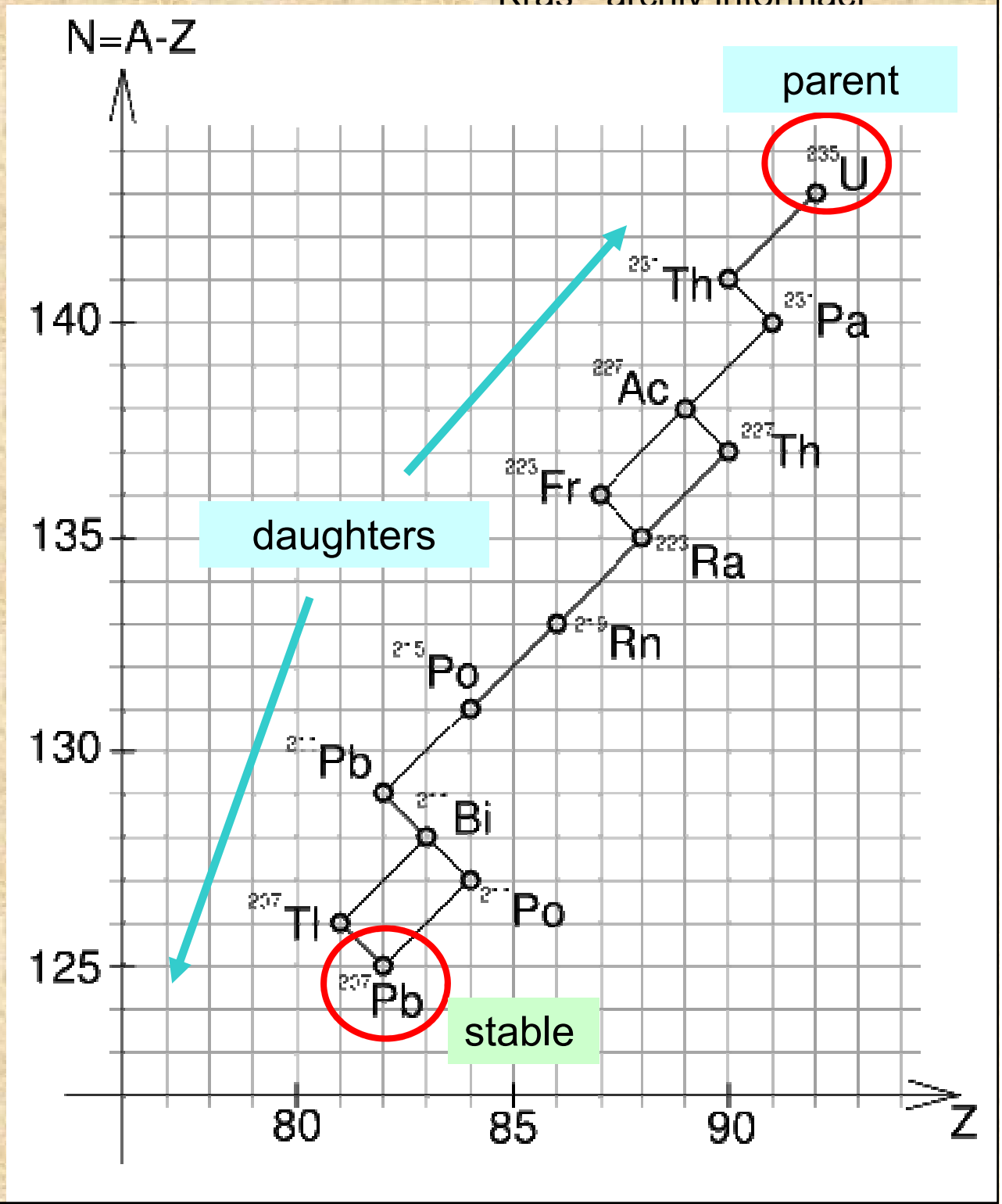

$^{232}Th \rightarrow {}^{208}Pb$

Izotop	Poločas přeměny	Přeměna	
^{232}Th	$1{,}405 \cdot 10^{10}$ r	α	
^{228}Ra	5,75 r	β^-	
^{228}Ac	6,15 h	β^-	
^{228}Th	1,9116 r	α	
^{224}Ra	3,66 d	α	
^{220}Rn	55,6 s	α	
^{216}Po	0,145 s	α	
^{212}Pb	10,64 h	β^-	
^{212}Bi	60,55 min	β^-	α (35,94 %)
^{212}Po	$0{,}299 \cdot 10^{-6}$ s	α	
^{208}Tl	3,053 min		β^-
^{208}Pb	*stabilní*		

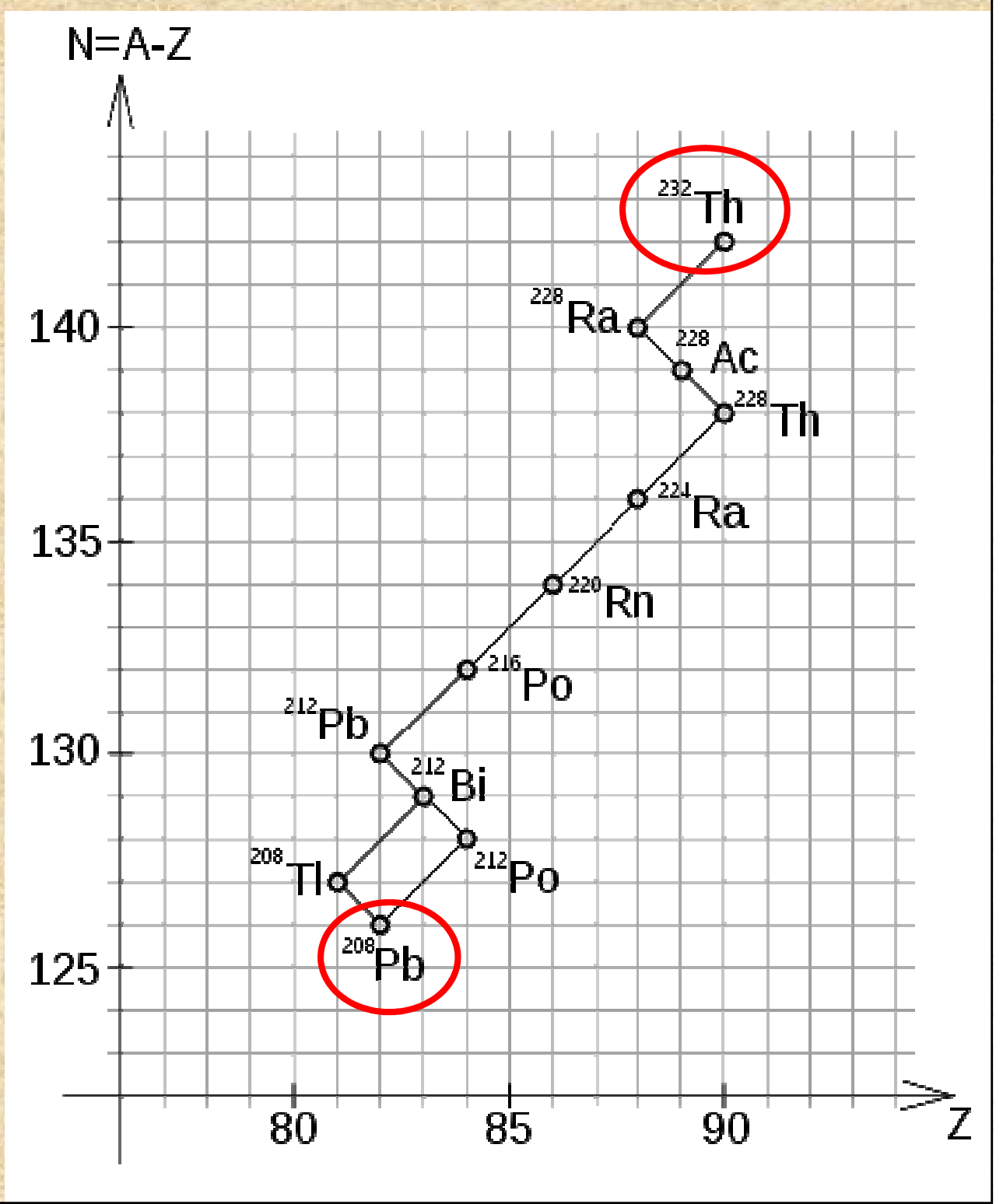

$^{238}U \rightarrow {}^{206}Pb$

Izotop	Poločas přeměny	Přeměna	
^{238}U	$4{,}468 \cdot 10^{9}$ r	α	
^{234}Th	24,10 d	β^-	
^{234m}Pa	1,17 min	β^-	
^{234}U	$2{,}455 \cdot 10^{5}$ r	α	
^{230}Th	$7{,}538 \cdot 10^{4}$ r	α	
^{226}Ra	1600 r	α	
^{222}Rn	3,8235 d	α	
^{218}Po	3,10 min	α	
^{214}Pb	26,8 min	β^-	
^{214}Bi	19,9 min	β^-	α (0,02 %)
^{214}Po	$164{,}3 \cdot 10^{-6}$ s	α	
^{210}Tl	1,30 min	α	β^-
^{210}Pb	22,20 r	β^-	
^{210}Bi	5,012 d	β^-	
^{210}Po	138,376 d	α	
^{206}Pb	*stabilní*		

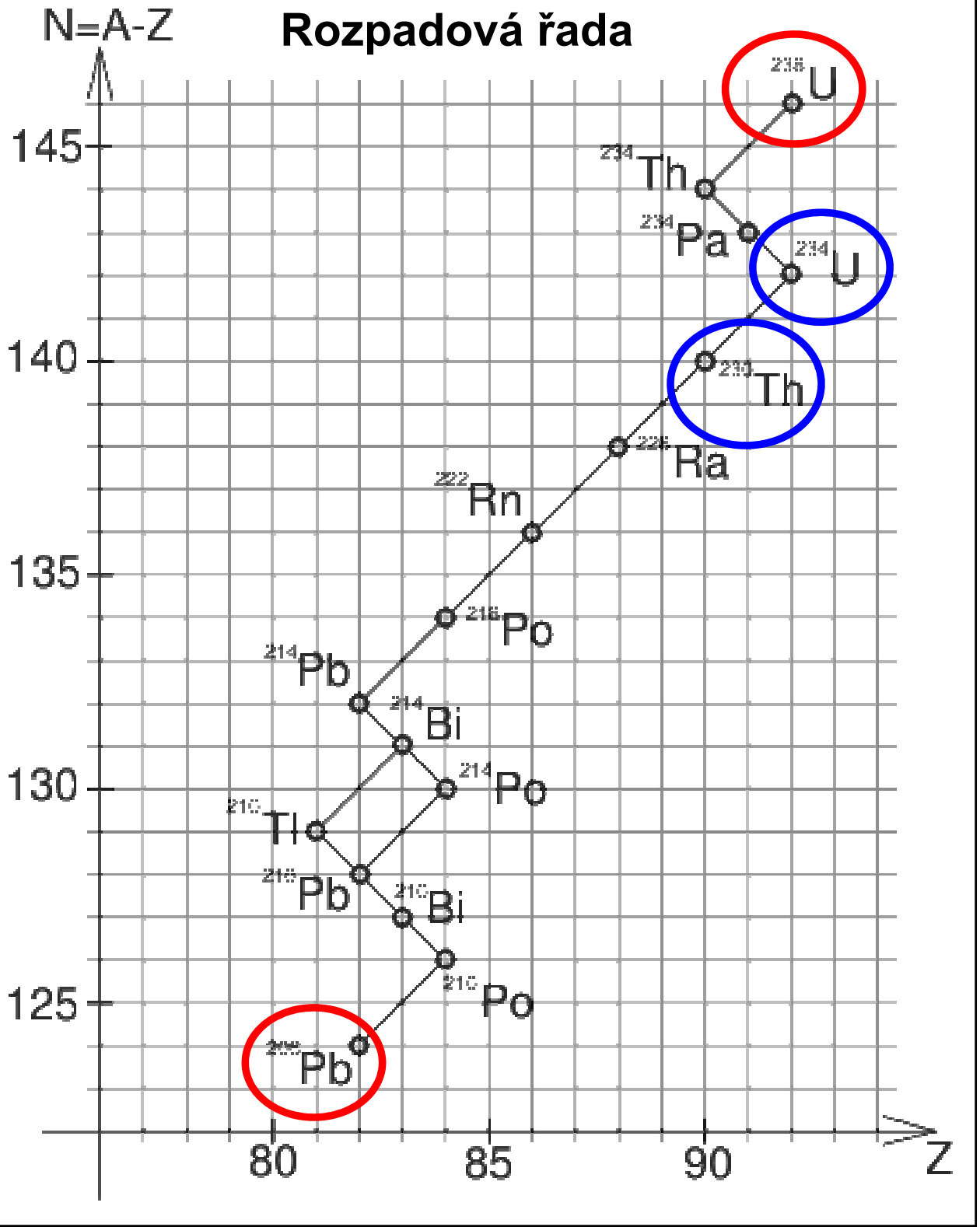

Datování - izotopická rovnováha

Datování pomocí izotopů U-Pb: stáří z přírůstku stabilních izotopů Pb, ^{206}Pb and ^{207}Pb, z rozpadu mateřských izotopů ^{238}U a ^{235}U.

Metody ^{238}U - ^{206}Pb, ^{235}U - ^{207}Pb, ^{232}Th - ^{208}Pb
Kombinace řad: metoda Pb-Pb

Radiometrické datování hornin a minerálů - pouze v případě, že byla ustavena izotopická rovnováha.

Radioaktivní/izotopická rovnováha (stacionární stav - rychlost vzniku a zániku dceřiných produktů je vyrovnaná)

V uzavřených systémech je **doba nutná k ustavení izotopické rovnováhy** v rozpadových řadách U a Th přibližně 400 - 500 ka (dolní hranice použití)!!!

Metody U-Pb a Pb-Pb použity pro datování starých karbonátů (Paleozoic and Mesozoic) (Moorbath et al. 1987).

Datování – mimo izotopickou rovnováhu

Daný pár radioizotopů dosahuje stacionární stav (radioaktivní rovnováhu) po době 5-násobku poločasu rozpadu dceřiného izotopu

$$\frac{dN_D}{dt} = \lambda_P N_P - \lambda_D N_D$$

$$N_P = N_P^{\,0}\, e^{-\lambda_P t}$$

přírůstek D = úbytek P

úbytek D - rozpad

$$\frac{dN_D}{dt} = \lambda_D N_D - \lambda_P N_P^{\,0}\, e^{-\lambda_P t} = 0$$

Integrace:

$$N_D = \frac{\lambda_P}{\lambda_D - \lambda_P} N_P^0 \left(e^{-\lambda_P t} - e^{\lambda_D t} \right) + N_D^0 e^{-\lambda_D t}$$

Obecné řešení pro rozpadovou řadu $\Rightarrow$ $N_P \rightarrow N_{D1} \rightarrow \ldots \rightarrow N_{Dn}$

$$N_{dn} = C_P\, e^{-\lambda_P t} + C_{D1}\, e^{-\lambda_{D1} t} + \ldots + C_{Dn}\, e^{-\lambda_{Dn} t}$$

$$C_P = \frac{\lambda_P \lambda_{D1} \ldots \lambda_{Dn-1} N_P^{\,0}}{(\lambda_{D1} - \lambda_P)(\lambda_{D2} - \lambda_P) \ldots (\lambda_{Dn} - \lambda_P)}$$

$$C_{Di} = \frac{\lambda_P \lambda_{D1} \ldots \lambda_{Dn-1} N_P^{\,0}}{(\lambda_P - \lambda_{Di})(\lambda_{Di+1} - \lambda_{Di}) \ldots (\lambda_{Dn} - \lambda_{Di})}$$

$$^{238}\mathrm{U} \xrightarrow[(4.49\times10^{9}\ \mathrm{yr})]{} {}^{234}\mathrm{U} \xrightarrow[(2.48\times10^{5}\ \mathrm{yr})]{} {}^{230}\mathrm{Th} \xrightarrow[(7.5\times10^{4}\ \mathrm{yr})]{} {}^{206}\mathrm{Pb}_{\mathrm{stable}}$$

The growth of daughter isotopes

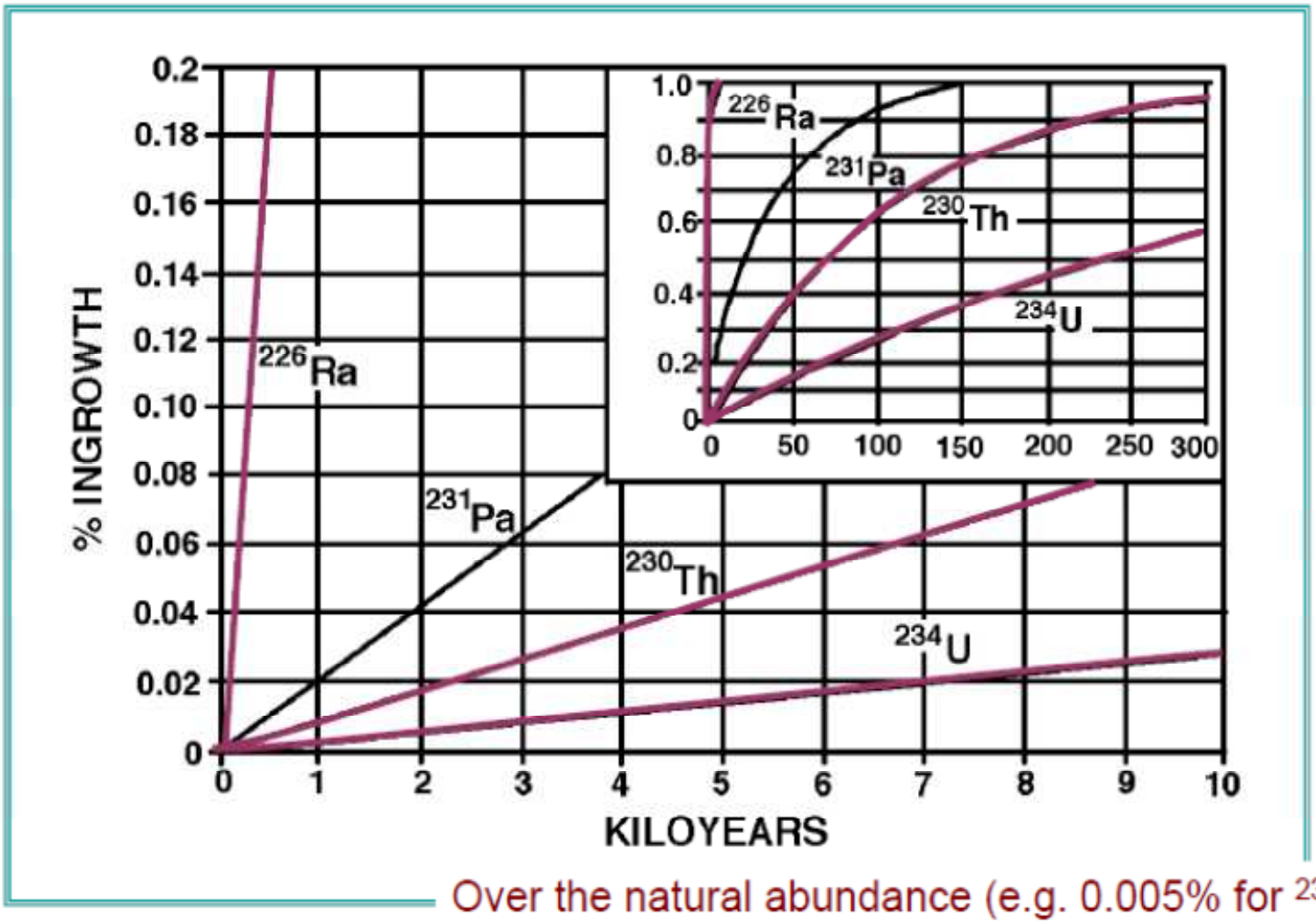

Over the natural abundance (e.g. 0.005% for ^{234}U)

Datování: pár Uran - Thorium

^{238}U - ^{234}U - ^{230}Th absolutní datovací technika

Využívá dynamiky vývoje alfa zářičů ^{238}U, ^{234}U a ^{230}Th.

- Poločas rozpadu ^{238}U je $t_{1/2} = 4{,}47.10^9$ let
- Poločas rozpadu ^{234}U je $t_{1/2} = 2{,}46 \cdot 10^5$ let
- Poločas rozpadu ^{230}Th je $t_{1/2} = 75{,}38.10^3$ let

Porovnání intenzit spektrálních píků uranu a thoria – umožňuje odhad stáří

Metoda může být použita, pokud je počáteční obsah ^{230}Th nulový

Datování speleotém

- Rozpuštěný uran ve skapové vodě (komplexy UO_2CO_3) – zabudovává se do kalcitové mřížky
- Thórium je v podstatě nerozpustné ve vodě – při tvorbě stalagmit žádné Th
- Nárůst ^{230}Th jako produkt rozpadu ^{238}U a ^{234}U je funkcí času

Datování U - Th

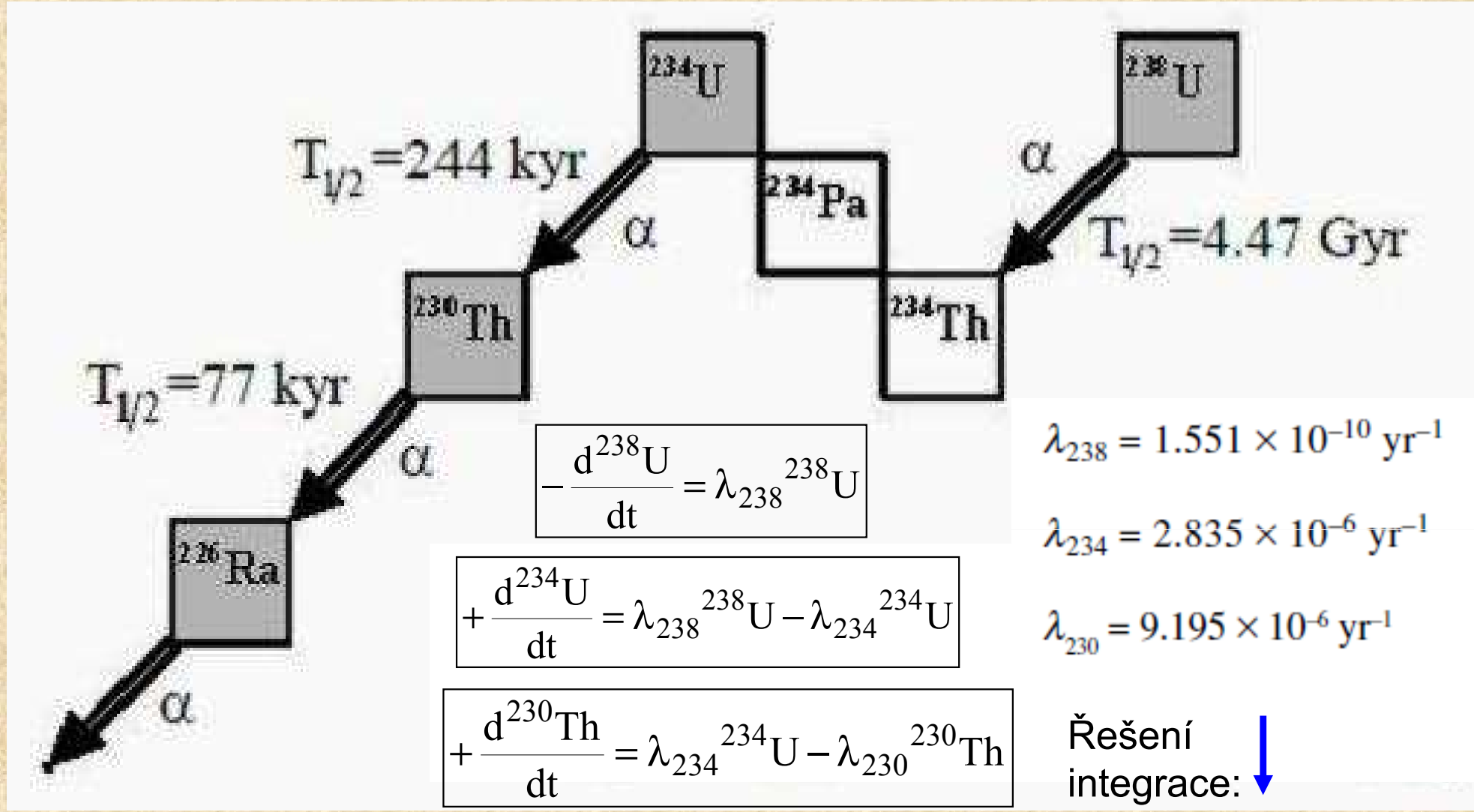

$$-\frac{d^{238}U}{dt} = \lambda_{238}{}^{238}U$$

$$+\frac{d^{234}U}{dt} = \lambda_{238}{}^{238}U - \lambda_{234}{}^{234}U$$

$$+\frac{d^{230}Th}{dt} = \lambda_{234}{}^{234}U - \lambda_{230}{}^{230}Th$$

$\lambda_{238} = 1.551 \times 10^{-10}\ \mathrm{yr}^{-1}$

$\lambda_{234} = 2.835 \times 10^{-6}\ \mathrm{yr}^{-1}$

$\lambda_{230} = 9.195 \times 10^{-6}\ \mathrm{yr}^{-1}$

Řešení integrace: ↓

$$\frac{^{230}Th}{^{234}U} = \frac{^{238}U}{^{234}U}\left(1 - e^{-\lambda_{230}t}\right) + \left(1 - \frac{^{238}U}{^{234}U}\right)\frac{\lambda_{230}}{\lambda_{230} - \lambda_{234}}\left(1 - e^{-(\lambda_{230} - \lambda_{234})t}\right)$$

Iterační řešení (numericky)

Rozpad izotopu ^{238}U

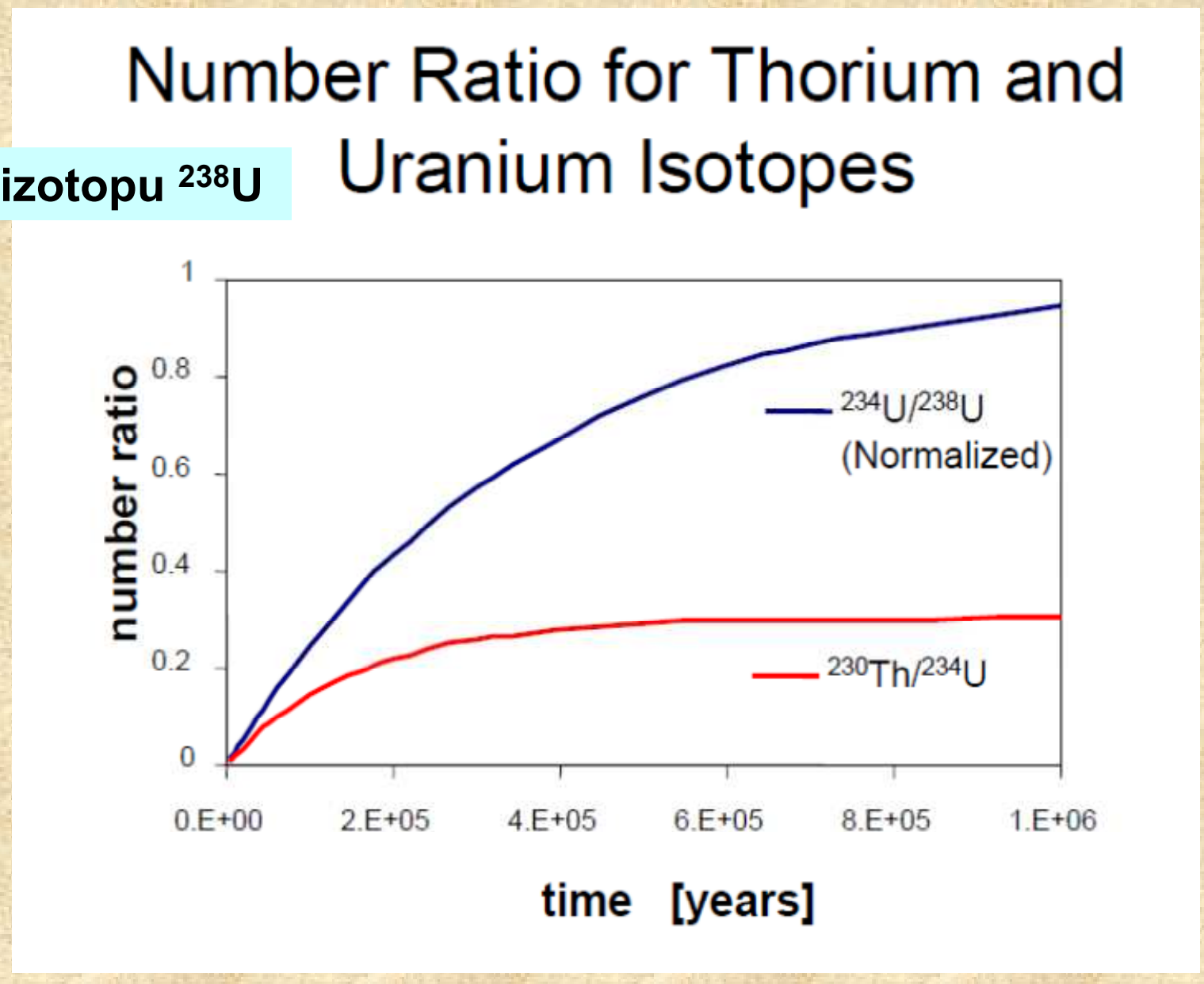

Poměr $^{234}U/^{238}U$ je konstantní v horninách (izotopická rovnováha). Je stejný ve vodách, které horniny rozpouštějí? Rostly speleotémy z vod s uniformním poměrem $^{234}U/^{238}U$?

Izotopická rovnováha v systému U - Th

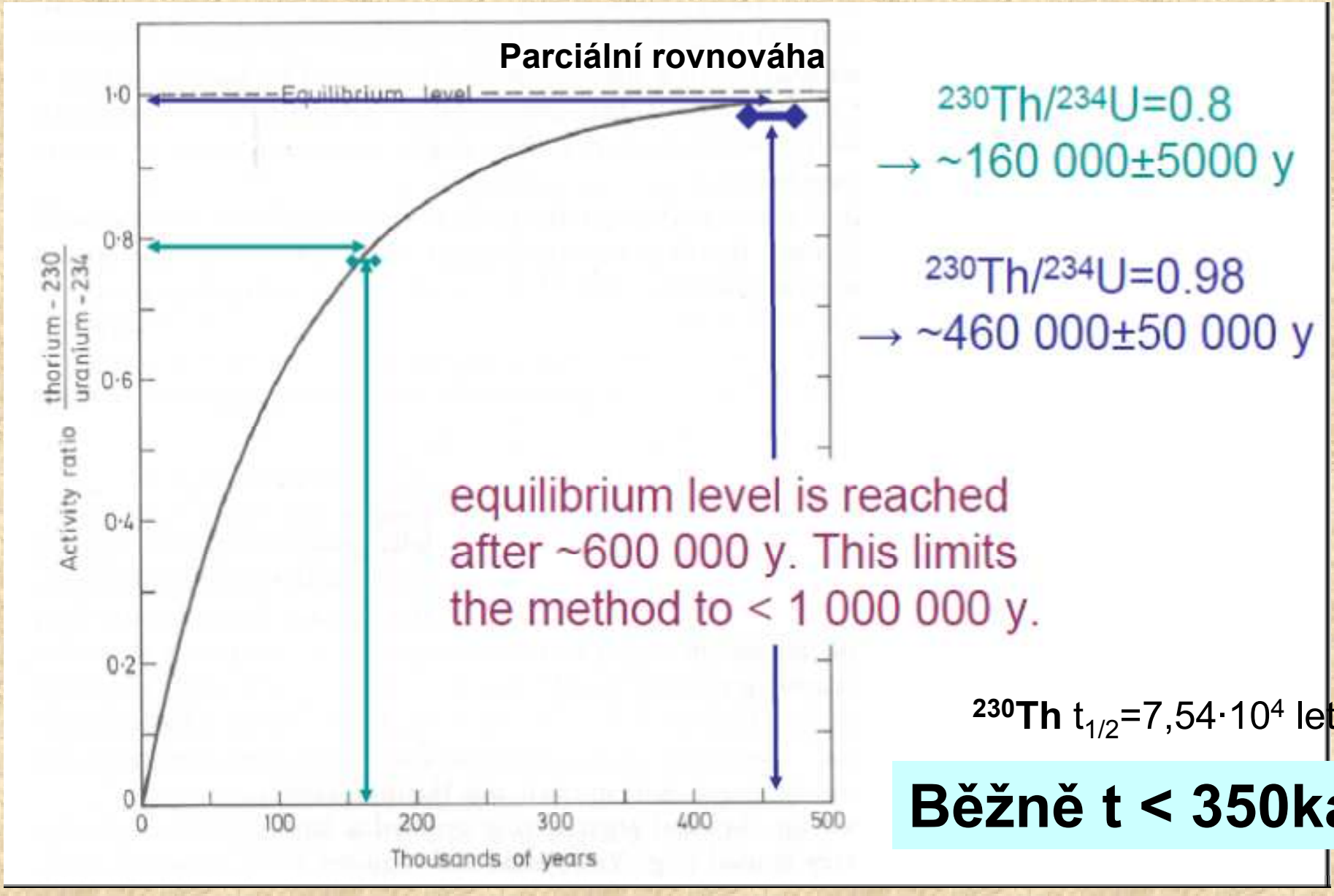

^{230}Th $t_{1/2}=7{,}54\cdot10^4$ let

Běžně t < 350ka!

Vzorky starší než 400,000 let budou mít stejný poměr ^{230}Th/^{238}U
Horní limit metody jako geochronometr

Další chronometry

Moderní hmotové spektrometry – přesnější měření za použití malých množství vzorků – pokrok proti předtím používanou α-spektrometrií (metodou počítání α-části) (Edwards et al., 1987).

Systém ^{234}U / ^{238}U jako geochronometr. Nerovnováha mezi **^{234}U a ^{238}U.**

Horní limit: 1.2 Ma díky delšímu $t_{1/2}$ ^{234}U.

Limitace: nejistota v počátečním poměru $^{234}U/^{238}U$.

Systém ^{235}U / ^{231}Pa jako geochronometr. Nerovnováha páru U/Pa v rozpadové řadě ^{235}U. Analogie $^{238}U/^{230}Th$ páru v sérii ^{238}U. Nezávislá kontrola (concordance checking) stáří vzorku (Edwards et al., 1997; Musgrove et al., 2001).

Horní limit: 200 ka (Chen and Yuan, 1988).

Modifikovaná U-Th metoda s nenulovým obsahem ^{230}Th na počátku (při vzniku speleotém)

$$\left(\frac{^{230}\mathrm{Th}}{^{238}\mathrm{U}}\right)_A = 1 - e^{-\lambda^{230}t}\left(1 - \left(\frac{^{230}\mathrm{Th}}{^{232}\mathrm{Th}}\right)_{A_0}\left(\frac{^{232}\mathrm{Th}}{^{238}\mathrm{U}}\right)_A\right) + \left(\left(\frac{^{234}\mathrm{U}}{^{238}\mathrm{U}}\right)_A - 1\right)\left(\frac{\lambda^{230}}{\lambda^{230} - \lambda^{234}}\right) \times \left(1 - e^{-(\lambda^{230} - \lambda^{234})t}\right)$$

kde $(^{230}Th/^{232}Th)_{A0}$ je poměr při vzniku vzorku (speleotémy)

$(^{232}Th/^{238}U)_A$ je měřená poměr (Cheng et al., 2000).

Radiokarbonové (^{14}C) datování

$$^{14}_{6}C = \quad ^{14}_{7}N + \beta^{-}$$

Nejužívanější metoda pro určení stáří terestrických o oceánských vzorků při studiu klimatických změn.

Její použití k chronologii speleotém je někdy považována za problematickou díky potenciální variabilitě v podílu tzv. „mrtvého uhlíku“ z vápencových hornin.

Podíl mrtvého uhlíku (***dead carbon proportion, dcp***)

obecně 10-20 % ale i vyšší hodnoty!

Podíl ***dcp*** závisí

(1) na stupni otevření systému

(2) na stáří půdní organické hmoty (Genty et al. 1999)

Nekorigované stáří určené metodou ^{14}C bývá v mnoha případech nadhodnoceno.

Navzdory problemům spojených s ^{14}C ve speleotémách, např. práce Beck et al. (2001) ukázala, že korekce dcp může za určitých okolností učinit radiokarbonovou metodu použitelnou.

Izotop ^{14}C nepřetržitě vzniká v **horních vrstvách atmosféry**

- výsledek interakce mezi neutrony kosmického záření a ^{14}N

$$^{14}_{7}N + ^{1}_{0}n = ^{14}_{6}C + ^{1}_{1}H$$

Předpoklad: produkce ^{14}C konstantní rychlostí!
Poměr radiogenního a neaktivního uhlíku v zemské atmosféře a oceánu (blízko povrchu) je konstantní: ~ 1 ppt (600 bilionů atomů/mol).

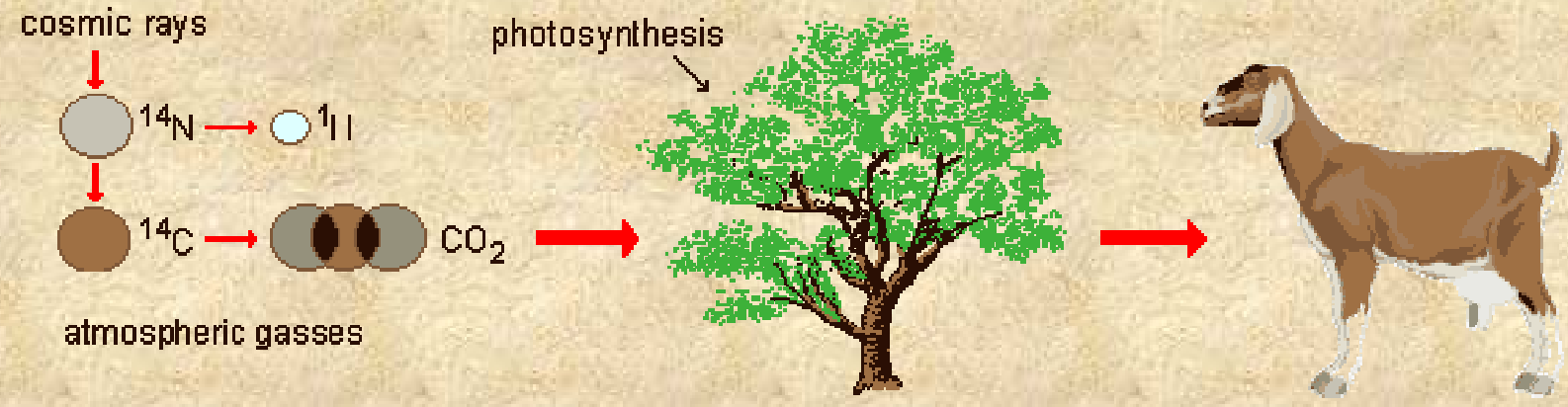

Atmosférický $^{14}CO_2$ je ***vázán rostlinami*** při fotosyntéze; poměr $^{14}C/^{12}C$ odpovídá poměru v atmosféře. Zvířata získávají ^{14}C z rostlin a dýcháním: ***všechny živé organismy mají poměr $^{14}C/^{12}C$ odpovídající poměru v atmosféře***

Specifická aktivita ^{14}C v biosféře téměř konstantní: 15,3 ± 0.5 d.p.m. / g C (decay per minute per g carbon)

Atomy ^{14}C se rozpadají podle rovnice: $^{14}_{6}C = {}^{14}_{7}N + \beta^-$

V mrtvé biotě poměr $^{14}C/^{12}C$ klesá díky rozpadu ^{14}C

Rovnice pro radioaktivní rozpad $\ln \frac{N_t}{N_0} = -\lambda t$, λ= 0.00012097 / yr (decay constant)

ze které $t = -\frac{1}{\lambda} \ln \frac{N}{N_0}$ $t = -8.035 \ln \frac{N_t}{N_0}$ $t = 19.035 \times 10^3 \log(N_0/N_t)$

(N/N_0 je poměr koncentrace ^{14}C ve vzorku a atmosféře

Poločas ^{14}C ($t_{1/2}$ = 5 730 let, $t_{1/2}$ = 5 568 ± 40 yr)

Limitní čas metody: << 100 000 roků

Srovnání dendrochronologického (přírůstky na kmenu stromů) a radiokarbonového stáří ukazuje ***fluktuace ^{14}C v atmosféře za posledních 10 000 let***.

Produkce ^{14}C nebyla vždy konstantní!

Výkyvy v atmosférickém radiouhlíku $\Delta^{14}C$ vzhledem ke standardu

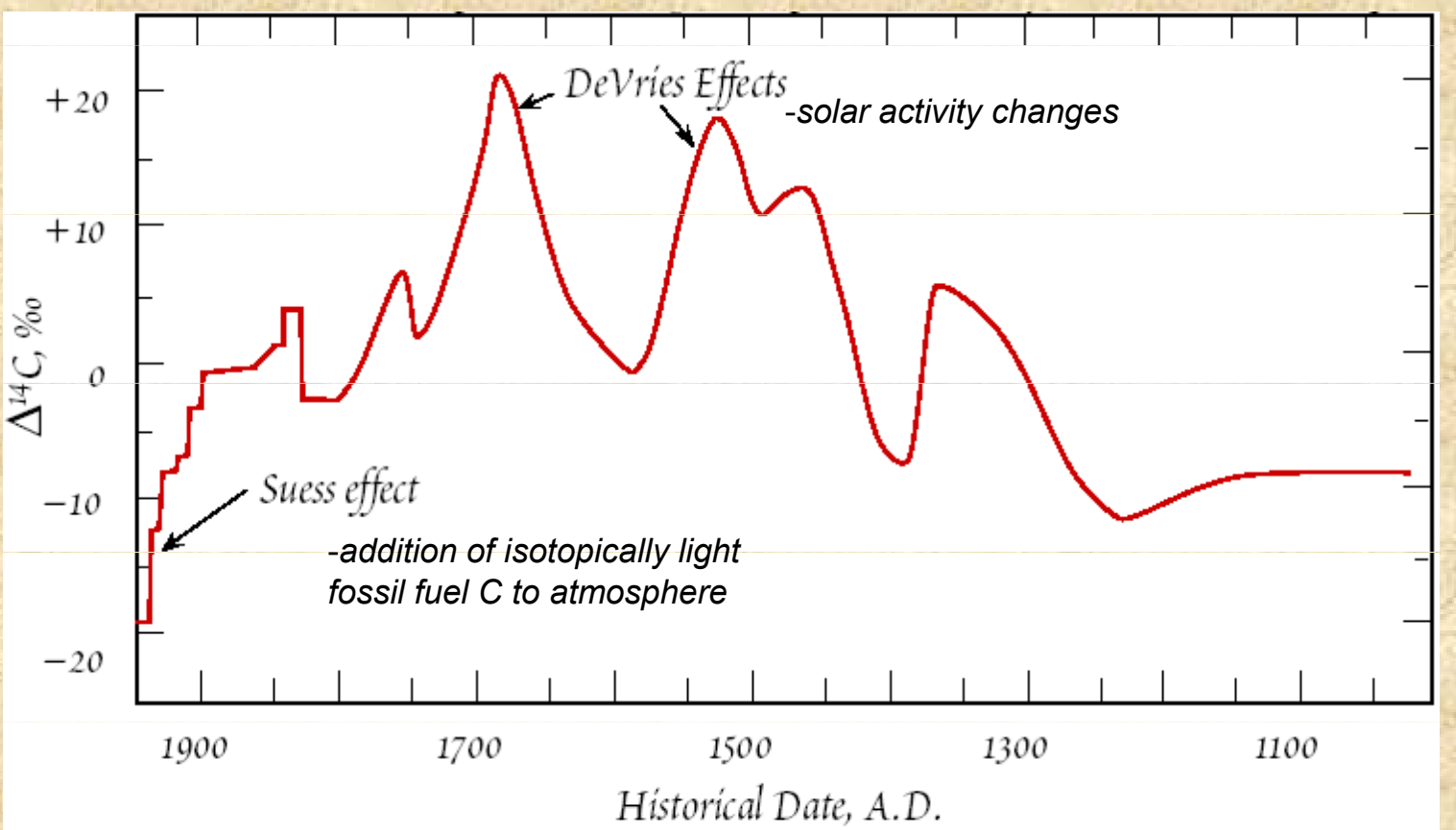

Figure 12.1. Variation of initial specific activity of ^{14}C in the past.

standard = kyselina šťavelová - odpovídá aktivitě ^{14}C ve dřevě z 1890
$\Delta^{14}C$ = **0** v roce 1890 (aktivita standardu).

Reconstructing atmospheric radiocarbon variability through time

What you need:
absolute age & radiocarbon age

$$A = A_0 e^{-\lambda t}$$

What you get:
history of $^{14}C_{atmos}$

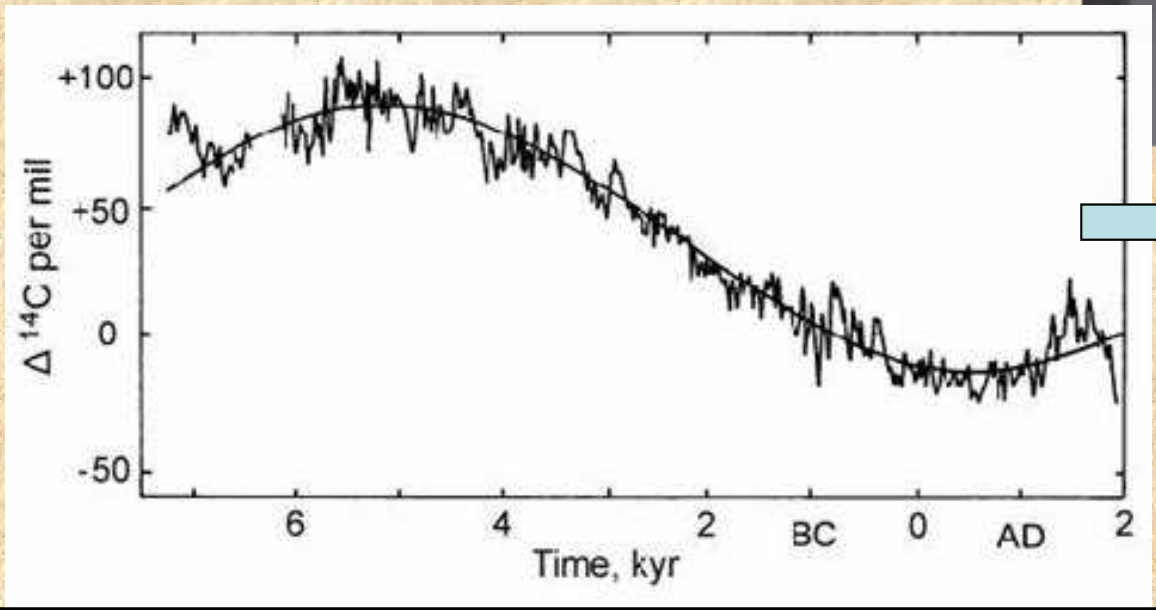

Most of the Holocene $^{14}C_{atmos}$ variability derives from changes in the geomagnetic field

The Radiocarbon Calibration Curve (atmospheric ^{14}C history)

Principle: compare radiocarbon dates with independent dates

examples of independent dating: tree-ring counting, coral U-Th dates, varve counting, correlation of climate signals in varves with ice core

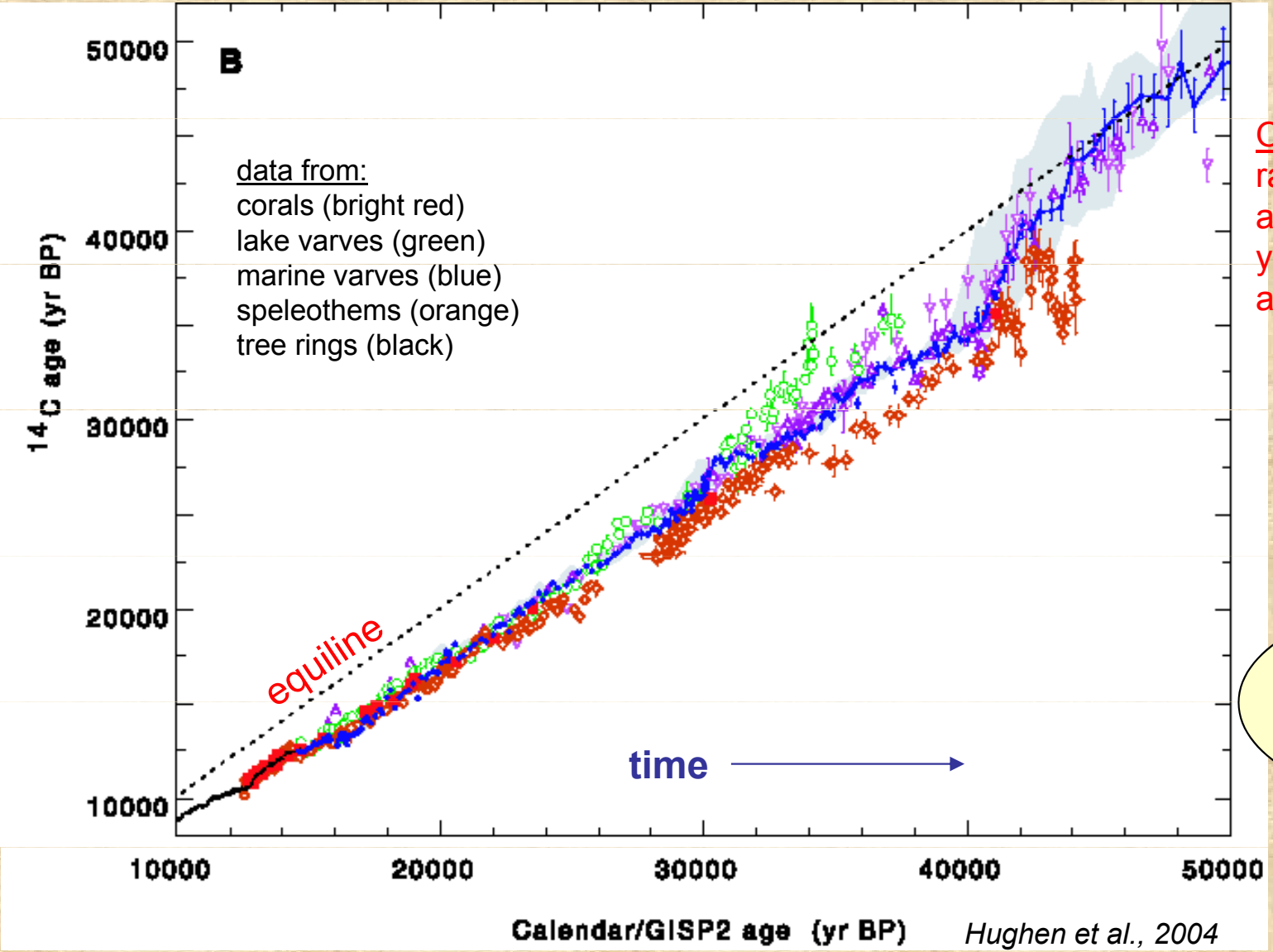

Hughen et al., 2004

Observation: radiocarbon dates are consistently younger than calendar ages

So was atmospheric ^{14}C larger or smaller at 20k (LGM) than today?

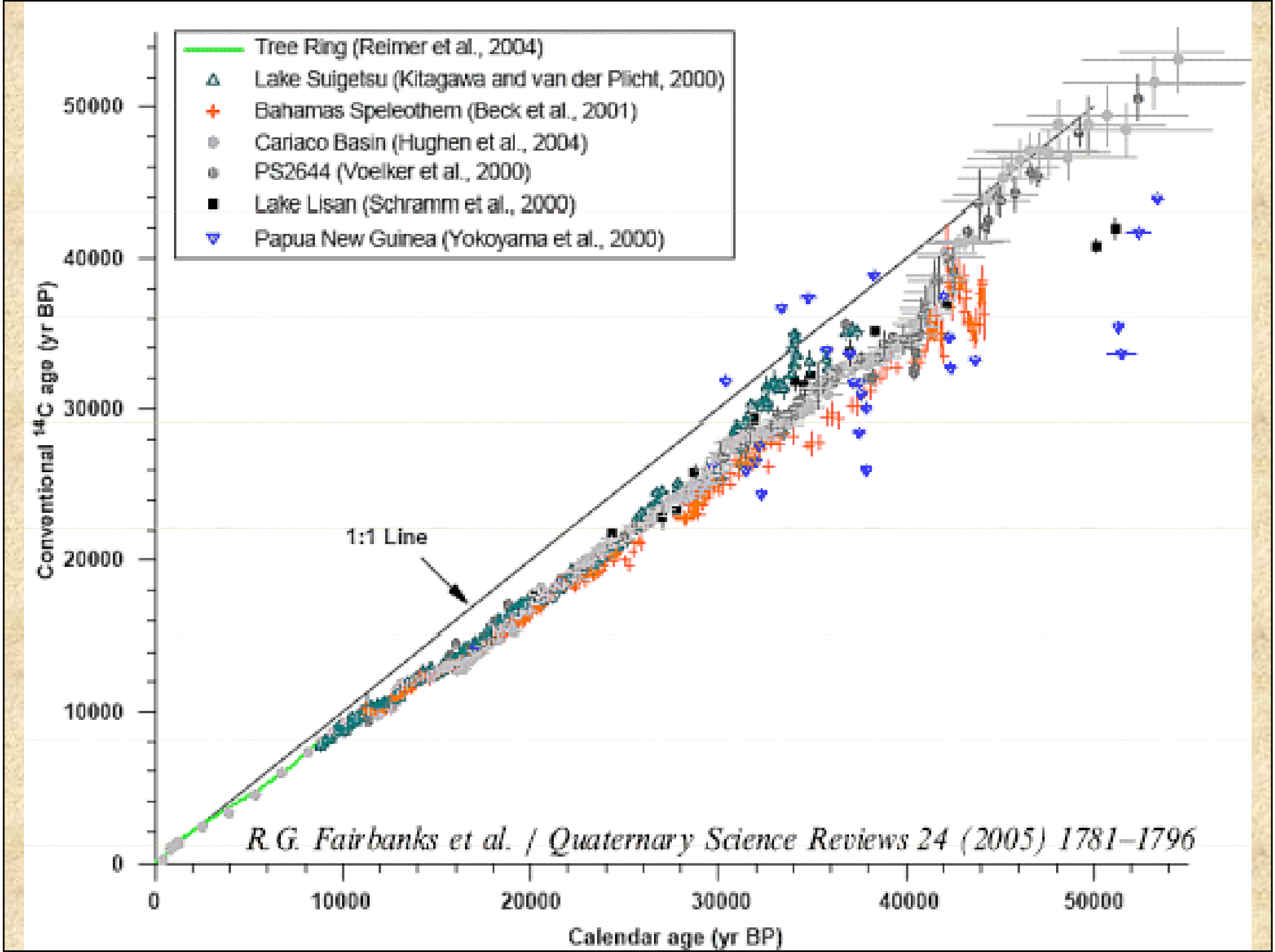
Tree Ring (Reimer et al., 2004)
Lake Suigetsu (Kitagawa and van der Plicht, 2000)
Bahamas Speleothem (Beck et al., 2001)
Cariaco Basin (Hughen et al., 2004)
PS2644 (Voelker et al., 2000)
Lake Lisan (Schramm et al., 2000)
Papua New Guinea (Yokoyama et al., 2000)
1:1 Line
Conventional ^{14}C age (yr BP)
Calendar age (yr BP)
0
10000
20000
30000
40000
50000
R.G. Fairbanks et al. / Quaternary Science Reviews 24 (2005) 1781–1796

Příklad datování pomocí ^{14}C

A sample of a living organism emits 15 particles per second. The same size sample of organic material found in an excavation emits 3.75 particles per second. What is the age of the sample BP and what was its age when first analyzed in 1993?

1. The half-life of ^{14}C is 5,730 years. $t_{1/2}$ = 5730
2. Since 3.75 particles per second are given in 1993 the half-life producing this result took 5,730 years.
3. Thus 5,730 years before 1993 the sample would have emitted 7.50 particles per second (2 X 3.75).
4. An additional full half-life would result in the organism emitting 15 particles per second (2 X 7.50 particles per second). This brings the age of the sample to 11,460 years (5,730 + 5,730).
5. Assuming a constant rate of decay the sample lived 11,460 years before 1993 since at that time it would have emitted 15 particles per second.
6. It should be dated to 11,417 BP (1993 - 1950 = 43 11,460 - 43 = 11,417)
7. Also it can be dated to BCE 9423 [1993 - 11,417 + 1 (since there is no year 0) = 9423]

KLIMATICKÝ ZÁZNAM V JESKYNÍCH

- **jeskynní prostředí je během desítek let víceméně konstantní.**
- **jeskyně – knihovna informací o událostech na povrchu v minulosti**
  - teplota je blízko ročních průměrných teplot regionu
  - události na povrchu řídí mocnosti výplní:
    - klastických sedimentů [(a)]
    - speleotém

[(a)] vodní hladina a průtok v blízkosti erozní báze variují v závislosti na srážkových událostech a povrchovém odtoku. Sedimentace a transport sedimentů je během roku proměnlivá. Ve vyšších patrech jeskyní jen malé změny (archiv událostí).

Informace ve speleotémách

Sekundární kalcitové výplně (sintry) obsahují:

1. Stopová množství uranu (umožňující datování)
2. Kalcitovou hmotu samotnou (ve spojení s datováním umožňuje odhad distribuce vápníku v průběhu času).
3. Variace/signál v izotovém složení ^{18}O (koreluje s teplotou)
4. Fluidní inkluze – vzorek původního roztoku ze kterého speleotémy rostly (zdroj informací o poměru $^{2}D/ ^{1}H$).
5. Organické povlaky (prstencové/vrstevnaté zbarvení) (zdroj informací o typu rostlin na povrchu).

Kras - archiv informací

Speleotémy, zejména **stalagmity a podlahové sintry**, rostou relativně pomale do značných rozměrů.

Válcovité stalagmity jsou nejlepší objekty na datování

- sekvence růstových vrstev v podélném řezu – "stratigrafie„
- válcové stalagmity rostou s konstantní rychlostí
- výška je úměrná stáří (času růstu)

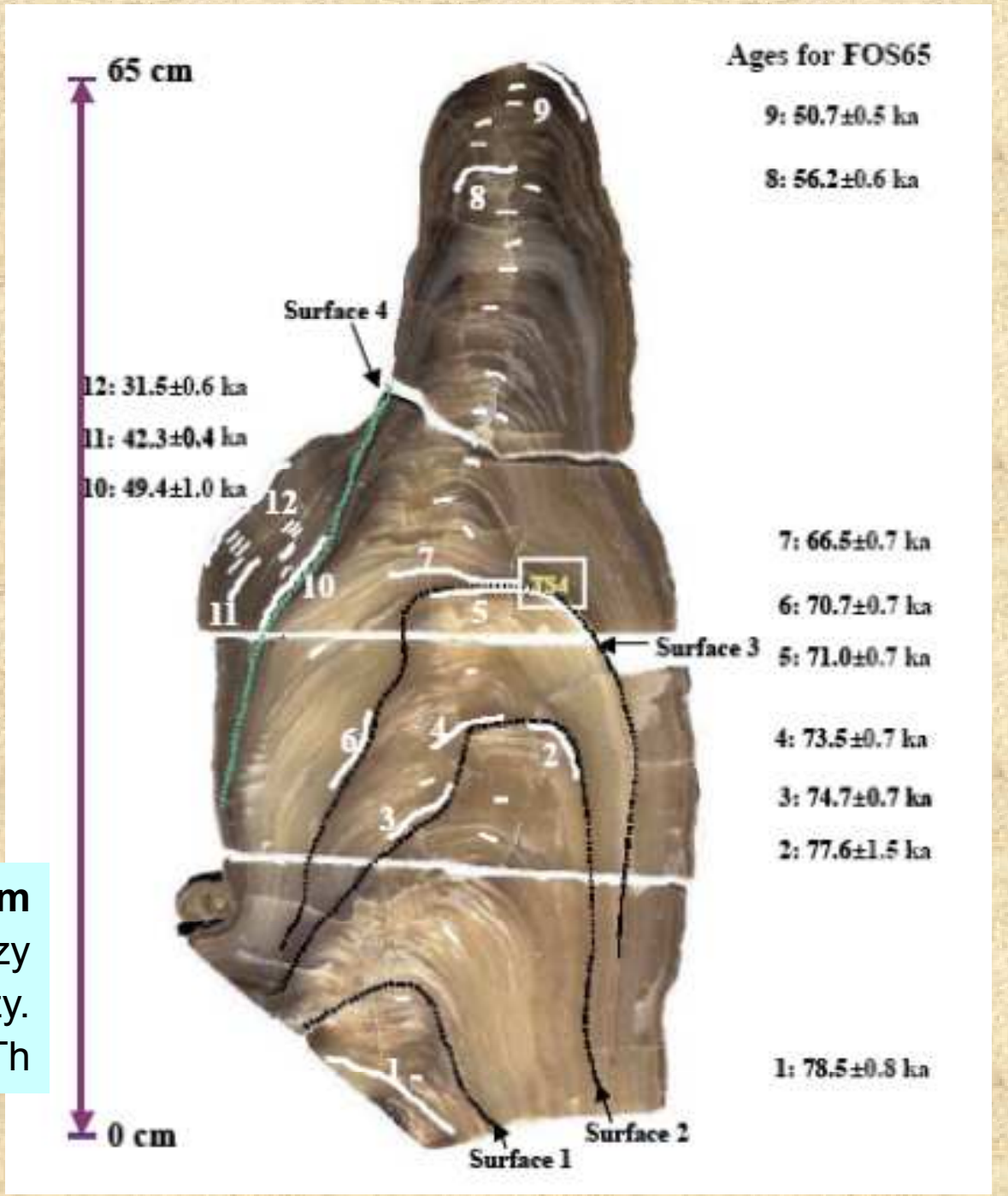

Řez stalagmitem
Dlouhé linie: geochem. analýzy
Krátké linie: izotopické analýzy.
Datování ^{238}U–^{234}U–^{230}Th

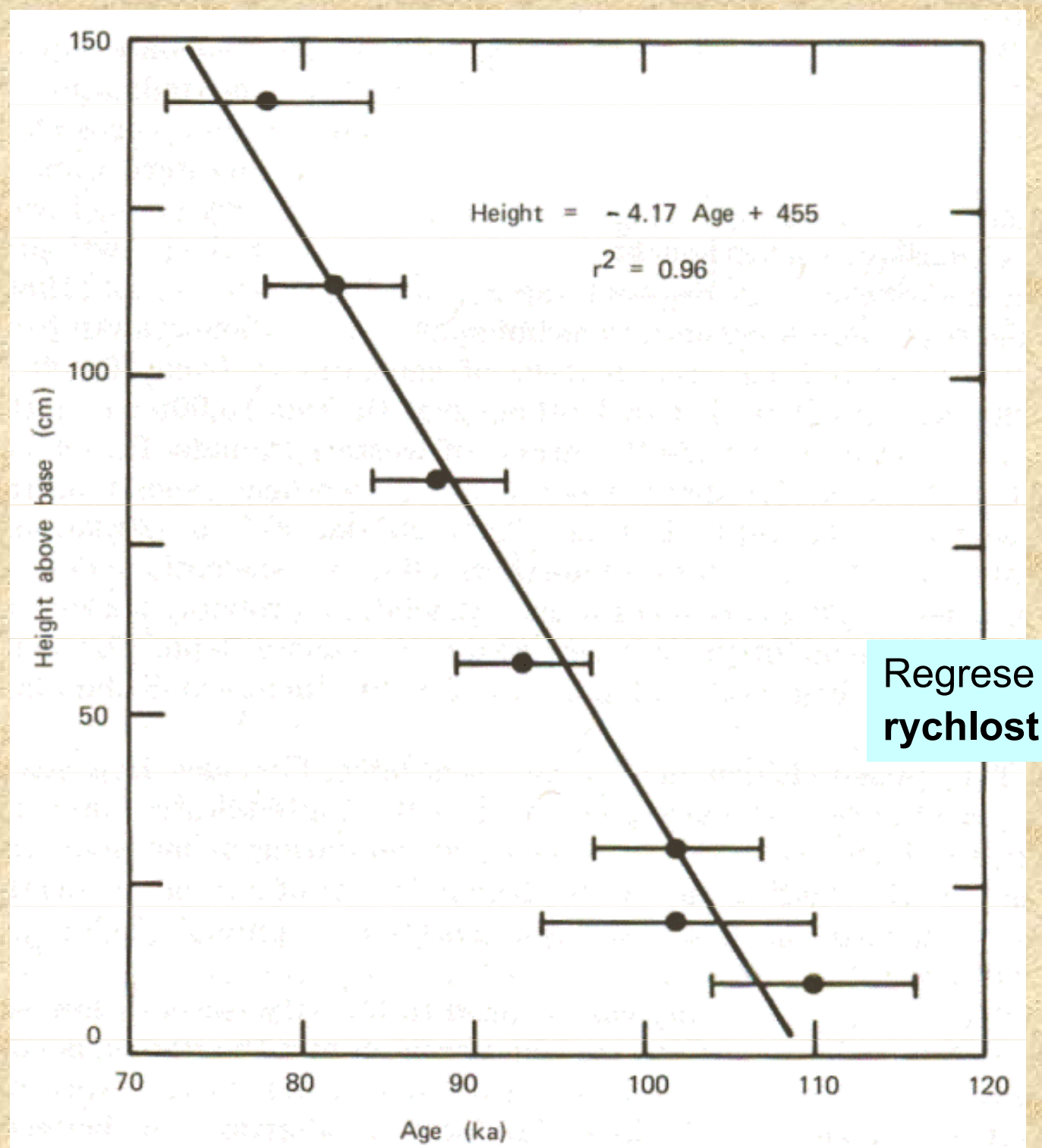

Křivka rychlosti růstu

Stalagmit, Little Trimmer Cave, Mole Creek Karst, Tasmania. Goede et al. (1986).

Regrese dat - směrnice závislosti
rychlost růstu: 4.17 cm/ka

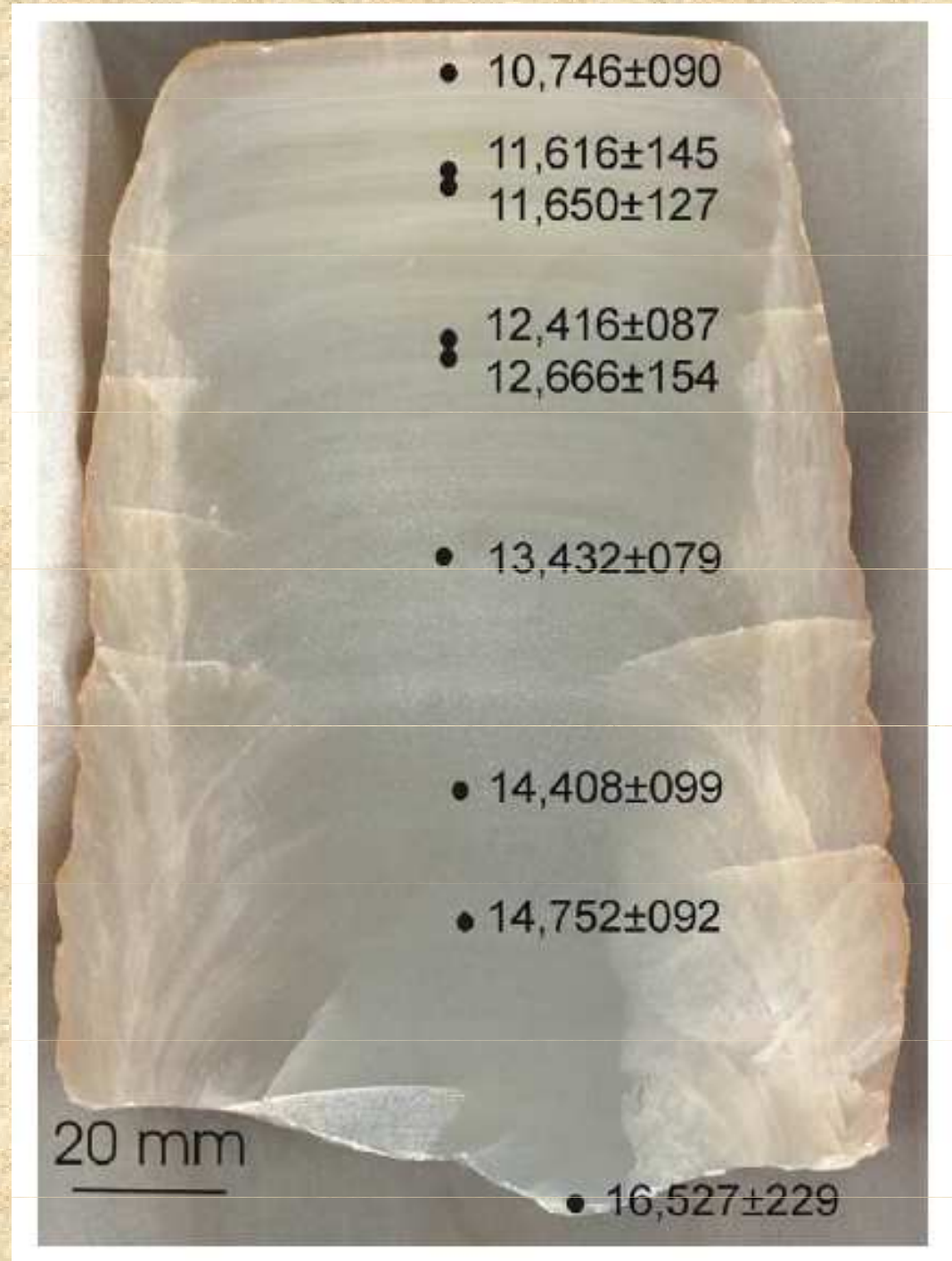

Photograph of the cross-section in stalagmite from Tangshan Cave indicating the ^{230}Th ***ages*** and 2σ errors in yr BP.

Další informace ze stratigrafie stalagmitů

Přechod masívních hrubě krystalických vrstev do tenkých páskovaných vrstviček, mezery obsahující prachovou/jílovitou frakci. **Informace u vlhkých a suchých obdobích?**

Páskované organické znečištění (proužky nebyly interpretovány)

- příliš mocné aby representovaly annuální cykly
- Možná cykly vlhkých a suchých období v rozmezí desítek až stovek let

Speleotémy s odlišných pater stupňovitých jeskyní mohou poskytnout minimální **stáří těchto pasáží**!

Bohužel, časové škály vývoje jeskyní jsou řádově větší než limit 350,000 let U/Th datování (nejčastější technika). Jen informce o nejčerstvějších událostech ve vývoji jeskynního systému a jeho snosové oblasti

Stáří speleotém v některých norských jeskyních byly tvořeny před Wurmským (Weichselian) zaledněním (Lauritzen and Gascoyne, 1980).

Reliktní pasáže jeskyní v Mendips a Yorkshire jsou starší než 350,000 let (Atkinson et al., 1978; Atkinson et al., 1984; Gascoyne et al., 1983b).

Datování stupňovitých vadózních jeskyní dovoluje odhad rychlosti zahlubování erozní báze. Rychlosti v Yorkshiru činily 50-200 mm/ka (Gascoyne et al., 1983a). Stáří dochovaných Yorkshirských údolí a jeskyní na 1 až 2 Ma.

Rozsáhlá data z datování speleotém z jeskyních různých oblastí a různých úrovní **mohou poskytnout informace, kdy se kalcit globálně ukládal a kdy ne**.

Kompilovaná data ze severní Anglie a západní Kanady (Gascoyne et al., 1983).

Jasně definovaná
- období masívního růstu
- období kdy růst byl zastaven.

Speleotémy - paleoklimatický záznam, severní Anglie a západní Kanada, Rocky Mountains resp. Mackenzie Mountains.
(Gascoyne et al. 1983).

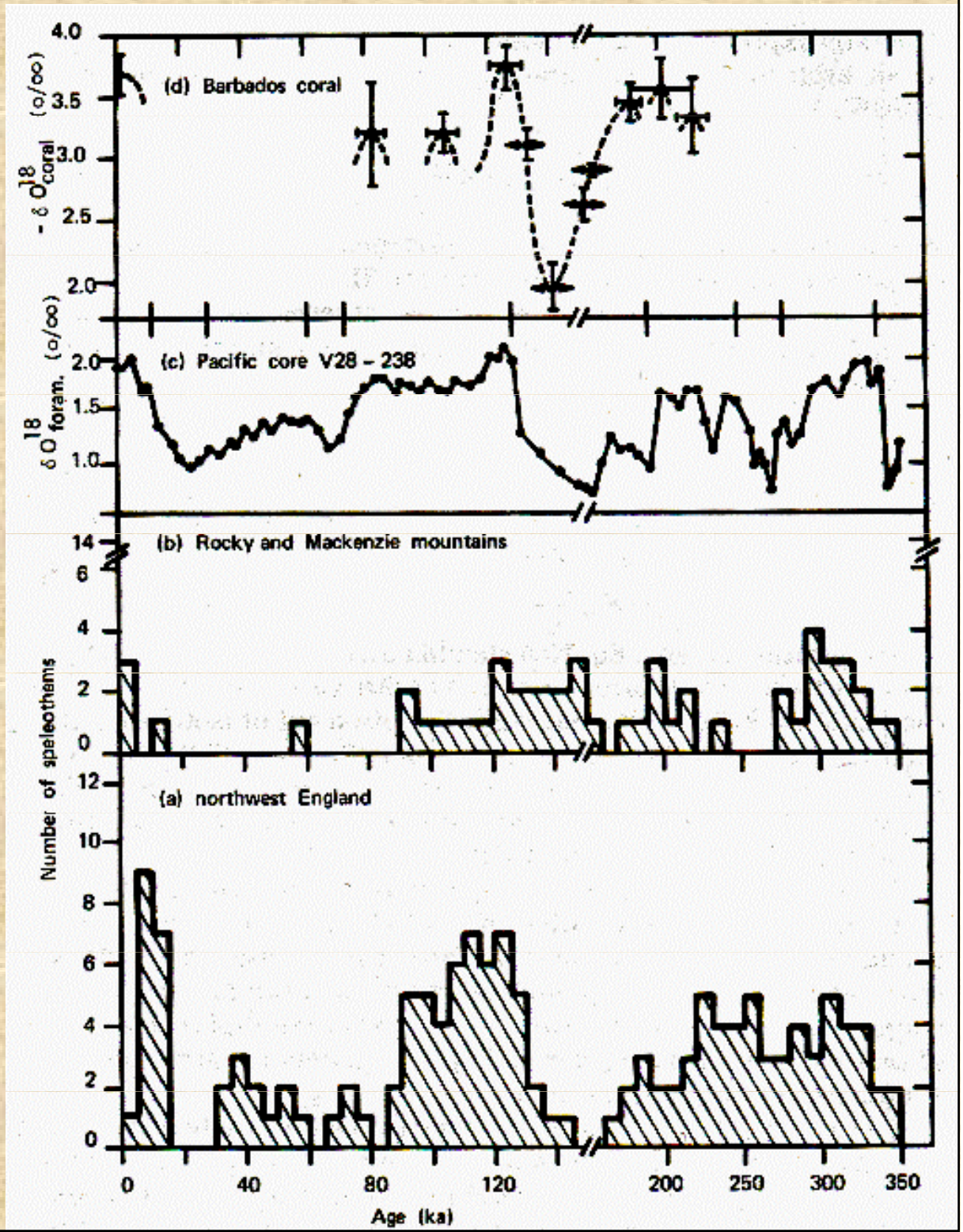

V severních klimatech

- **růst speleotém ustává během zalednění**, pravděpodobně díky permafrostu
- intenzívní růst speleotém v interglaciálech s mírným klimatem a hojnými srážkami.

Anglie a Skotsko:

- nepřetržitý avšak řídký růst speleotém 40 – 26 ka
- **absence speleotém 26 – 15 ka**
- hojný růst speleotém od 15 ka - dnešek (Atkinson et al., 1986)

Mackenzie Mountains, západní Kanada:

5 odlišných období **růstu speleotém**:

- 15 ka – dnešek
- 150 - 90 ka
- 235 - 185 ka
- 320 - 275 ka
- starší než 350 ka (Harmon et al., 1977)

V aridních oblastech v nižších zeměpisných šířkách opak!

- Růst speleotém v aridním jihozápadě USA je spojený Pleistocenními dešťovými obdobími.
- Radiokarbonové datování masivních stalagmitů v Rössing Cave, Namibijská poušť, Afrika, datuje růst k Wurmskému (Weichselian) pluvial (Heine and Geyh, 1983).

Datování speleotém může být použito k **určení hladin moře v minulosti**.

- Podvodní jeskyně na Bermudách a Bahamách obsahují speleotémy, které byly formovány v době, kdy jeskyně byly nad hladinou moře.
- Stalagmity na Andros Island (Bahamy) rostly mezi 160 000 a 139 000 lety
- Souvislost se zaledněním (Illinoian glacial) (Gascoyne, et al., 1979).

Kras - archiv informací

The isotopic composition of groundwaters and precipitates from groundwaters varies depending on the processes of dissolution and precipitation and the temperatures at which these processes occur. Making use of the temperature dependence, isotopic compositions, particularly *IBO/60* and 2H/H, are widely used as paleothermometers. Because the changes in isotope ratio are very small, they are generally expressed in delta units as parts per thousand with respect to an arbitrary standard known as standard mean ocean water (SMOW)

$$\delta(\text{o/oo}) = 1000\,\frac{R - R_{\text{SMOW}}}{R_{\text{SMOW}}}$$

Measurements using modern mass spectrometers are accurate to ± 0.2 percent for 180 and to ±2 percent for 2H.
Use of oxygen isotope ratios as a paleothermometer depends on isotopic equilibrium between the seepage water and the precipitating calcite:

$$\frac{(^{18}O/^{16}O)_c}{(^{18}O/^{16}O)_w} = K_{cw}(T)$$

The temperature is then calculated from the temperature dependence of *K* (Harmon et al., 1977):

$$10^3 \ln K_{cw} = 2.78 \times 10^6 T^{-2} - 2.89$$

If precipitation is slow, Eq. 10.5 should be satisfied. The test (Hendy, 1971) is to compare variations in 180 with variations in l3C.Their correlation is evidence for rapid precipitation out of isotope equilibrium as has been claimed (Fantidis and Ehhalt, 1970). However, most recent studies do not find this correlation, and the authors have proceeded with temperature calculations (Thompson et al., 1976; Harmon et al., 1977; Harmon, 1979).
If the speleothem oxygen isotope ratio is to record cave temperature at the time of deposition, which in turn is to measure mean annual temperature at the land surface, it is necessary that the isotopic ratio not depend on annual fluctuations in rainfall and surface temperatures. Yonge et al. (1985) show that the isotopic composition of seepage waters is constant and approximately equal to the mean annual precipitation of the area.

To solve Eq. 10.5, one needs isotope ratios for calcite and for the seepage water. The calcite can be measured but the preserved specimens of seepage water in the fluid inclusions may have undergone oxygen isotope exchange with the enclosing calcite, invalidating the measurement. A linear relation, known as the meteoric water line, exists between oxygen and hydrogen isotopes for surface waters. Comparison of the 180 determined from the calcite with deuterium determined from the fluid inclusions (Fig. 10.11) shows that the seepage waters follow the meteoric water line closely. Thus, deuterium from the fluid inclusions, which should not have isotope exchanged with the enclosing calcite, can be used to calculate the corresponding 180 of the seepage water; this allows paleotemperatures to be calculated. The 180 ratios in present-day cave seepage waters correlate directly with cave temperatures (Fig. 10.12). Cave temperature is a good measure of mean annual surface temperature, and the oxygen isotope composition is a good measure of the isotope composition of rainfall.

The combination of ThjU dating of speleothems with their 180 and 2Hcompositions as a paleothermometer allows the construction of temperature-time curves for regions where appropriate quantities of cave deposits exist. Speleothems become the continental equivalent of the deep-sea cores that have established much of the Pleistocene climatic record (Gascoyne et al., 1980; Gascoyne et al., 1981; Harmon et al., 1978a; Harmon et al., 1979; Schwarcz et al., 1976). The complete establishment of a North American climatic record is underway, but because of the large range of space and time, many more data points are needed before the climatic picture at various times in the late Pleistocene comes into focus.

Clastic Sediment Records and Paleohydrology

The in-fillings of clastic sediments depend on how cave passages are disposed with respect to the sediment sources, but they also depend on high-velocity flow to transport clastic material. The required flows, interpreted in terms of the hydrogeologic setting of the cave, tell something about climatic conditions at the surface, particularly about total precipitation and how precipitation is distributed. Long periods of continuous but low-intensity rainfall produces a response in the cave system quite different from that produced by the same total precipitation appearing as episodic but very intense storms.

Among sedimentary deposits that have been described are the following:

1. Cobble and boulder fills, unbedded and unsorted, that require occasional intense flood flows to transport and emplace.
2. Bedded silts, sands, and fine gravels representative of highvelocity stream flow.
3. Massive unctuous clays that may have settled under static water conditions with the cave acting as a "settling tank."
4. Fine-grained laminated clays that look much like varved clays found in lakes and that may represent pulses of sedimentladen water moving into flooded passages (Bull, 1981; Gillieson, 1986).

All cave sediments in the active portions of caves are only in temporary residence. What appear to be passive sediment beds can be removed en mass in episodic floods, only to be replaced with other sedimentary material as part of the continuous sediment flux through the karst drainage system. Those sediments that happen to be in residence when the passages are drained for the last time are preserved when the passage moves from the enlargement to the stagnation stage. There has been little success (see Section 8.4) in discovering any sort of continuous beds that can be traced laterally for long distance. However, the form of the deposits gives some clues about the flow conditions that existed when the passage was last abandoned.

If passages with measurable cross sections (not too much of the passage obscured by sediments) and uniform scalloping can be found, then the paleodischarge can be calculated. If the catchment area can be identified and its boundaries are reasonably certain, then a paleorunoff intensity can be calculated and compared with presentday conditions in the same basin.

Time scales for the **Tertiary and Quaternary periods**. Subdivisions of the Quaternary are given for North America and for northern Europe [Extracted from Van Eysinga (1983)]

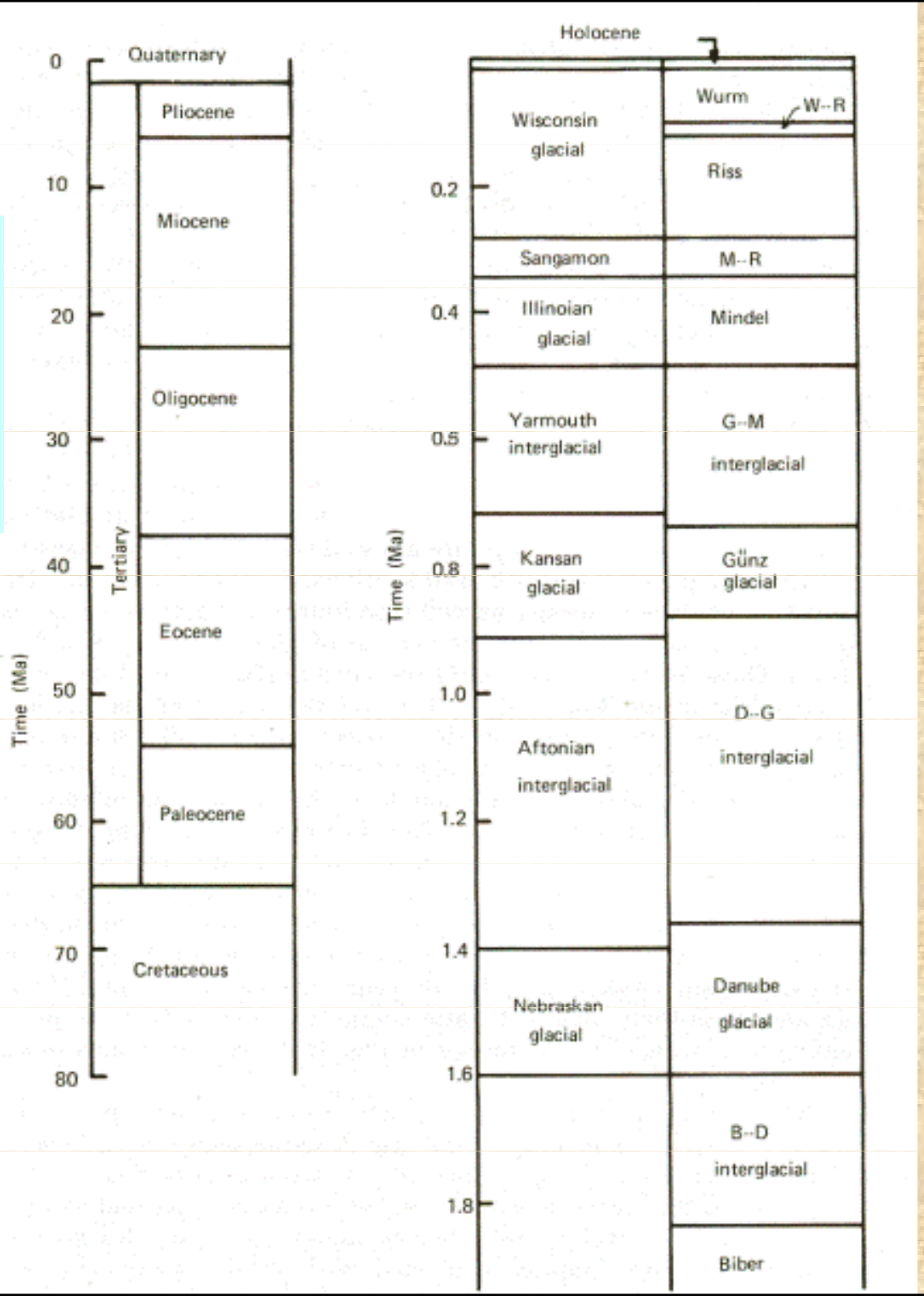

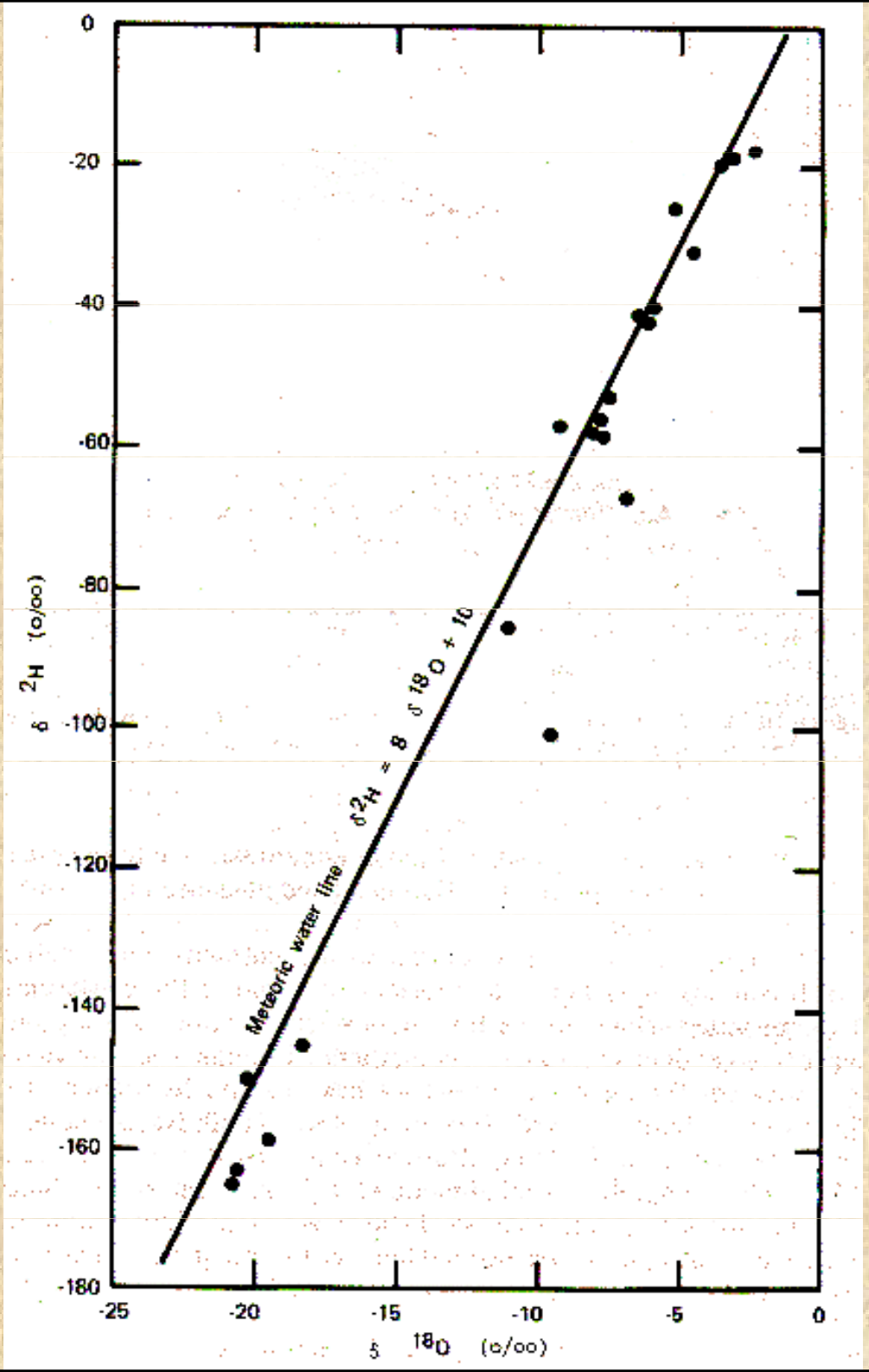

Data for various cave-seepage waters (Yonge, et al., 1985) compared with the meteoric water line. Both $^{18}0$ and ^{2}H shifts were measured with respect to SMOW.

Kras - archiv informací

Dependence of $\delta^{18}0$ on temperature for seepage waters in various caves in North America. Data are from Yonge et al. (1985).

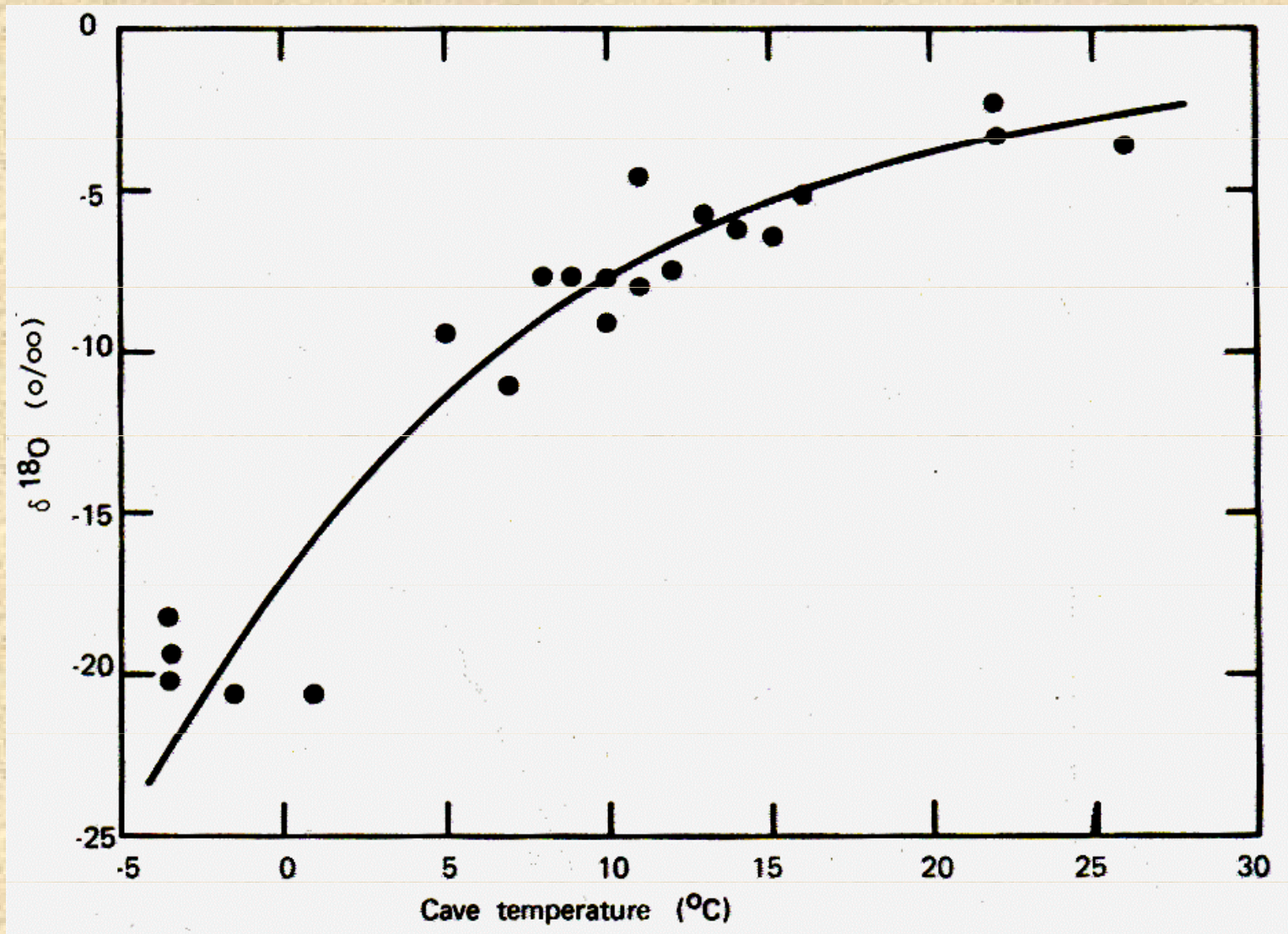

Kras - archiv informací

Kras - archiv informací

Carbon-14 Dating

Cosmic rays striking the upper atmosphere convert ^{14}N to ^{14}C at a rate that can be assumed to have been constant over time. Atmospheric mixing brings the 14C,with a half-life of 5730 years, into the lower atmosphere, where it forms a constant mixture with the stable ^{12}C and ^{13}C isotopes.

A tree, for example, draws CO_2 from the atmosphere as it grows, and the living wood contains the background concentration of ^{14}C. When the tree dies or is burned, leaving residual charcoal, the exchange of carbon with the atmospheric reservoir is terminated and the incorporated ^{14}C begins to decay. By measuring the ^{14}C content of an old carbon, one can calculate the time elapsed since the cutoff from the atmospheric reservoir occurred. In this manner, ages of carbon-containing specimens can be determined up to a limit of about 50,000 years.

In principle, 14C dating methods can be applied to young speleothems, providing the source of carbon in the speleothem can be identified.

The main source of dissolved carbonate in the seepage waters that deposit travertine is the dissolution of limestone bedrock at the soil/bedrock interface by carbonic acid derived mainly from the soil atmosphere. From the chemical reaction (10.1)

$$CaCO_3 + CO_2 + H_2O \rightleftharpoons Ca^{2+} + 2\,HCO_3^- \qquad (10.1)$$

one would expect the calcite-depositing waters to be composed half of recent carbon from the soil and half of "dead" carbon from the limestone. Actual measurements of freshly deposited cave calcites (Broecker and Olson, 1959) give an isotope ratio with 70 percent ± 20 percent modern carbon. This circumstance extends the potential dating period back to about 30,000 years, but it also requires that one know the fraction of modern carbon in the original deposit.

Isotope exchange during dissolution and redeposition appears to upset the carbon balance implied by Eq. 10.1.

The best approach is to select calcite depositional sequences such as stalagmites or cores through flowstone cascades, where the "top„ of the sequence is still growing. From analysis of the zero-age material, the 14Cdeficit, and thus an age correction, can be determined which can then be applied to the lower parts of the section. The only assumption is that the fractionation processes have been constant over the period of deposition.

Datování pomocí rozpadové řady uranu (Uranium-Series Dating)

The most abundant isotope of uranium, ^{238}U undergoes a long decay scheme (Fig. 10.4) ultimately to the stable ^{206}Pb. An intermediate step in the decay scheme is ^{234}U with a half-life of 2.45×10^5 years before it decays to ^{230}Th. Likewise, the minor isotope ^{235}U undergoes decay through ^{231}T hand ^{231}Pa on its way down the decay chain.

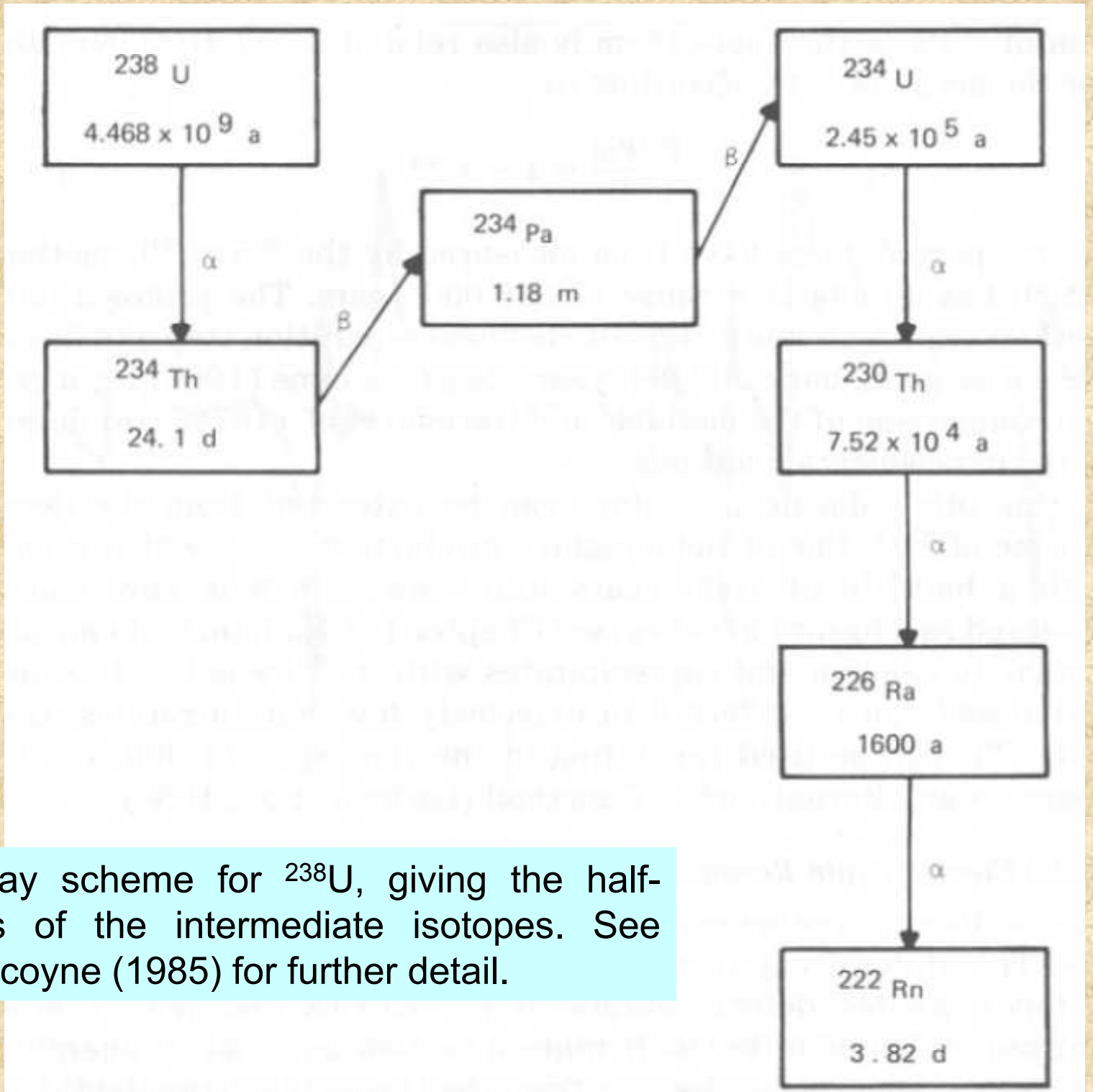

Decay scheme for ^{238}U, giving the half-lives of the intermediate isotopes. See Gascoyne (1985) for further detail.

To the convenient half-lives of ^{234}U and ^{231}Pa is added a quirk of geochemistry that turns these decay sequences into a useful dating method for speleothems. Thorium occurs in nature only as the ThH state, which forms oxides, silicates, and phosphates that are extremely insoluble.

Although Th-containing minerals such as zircon and monazite are found in clastic sediments in caves, there is essentially no thorium in groundwater.

Uranium, in the oxidizing environment of karst groundwater appears as the six-valent UO_2^{2+} ion, which is further solubilized by complexing with carbonate. Uranium is readily transported as $UO_2(CO_3)_2^{2-}$ and $UO_2(CO_3)_3^{4-}$ species and secondary calcite deposits commonly contain a few parts per million of uranium.

For a speleothem to be datable, it must

1. Contain some uranium (0.1 ppm or more).
2. Be free of detrital material containing thorium.
3. Be nonporous and have not undergone recrystallization at any time since the calcite was deposited.

The technique now widely used for speleothem age dating consists of the following steps:

The speleothem is dissolved, spiked with a known quantity of ^{232}U and ^{228}Th to act as an internal standard, purified, and the uranium and thorium are separated by ion exchange.

These elements are then extracted and plated out on steel disks, and the alpha-spectrum is determined.

Integrated areas under the alpha-peaks are directly proportional to the activity of each isotope.

Three different dating calculations are possible: $^{230}Th/^{234}U$, $^{234}U/^{238}U$ disequilibrium, and $^{231}Pa/^{235}U$ combinations.

Because thorium is insoluble and not transported into the growing speleothem, it is assumed that any thorium that appears in the analysis is a result of the decay of ^{234}U. Because of the sequence of somewhat similar halflives, the age relationship is

$$\frac{[^{230}Th]}{[^{234}U]}t = \frac{1 - e^{-\lambda_0 t}}{[^{234}U/^{238}U]} + \frac{\lambda_0}{(\lambda_0 - \lambda_4)}\left(1 - \frac{1}{[^{234}U/^{238}U]}\right)(1 - e^{-(\lambda_0 - \lambda_4)t}) \quad (10.2)$$

where λ_0, λ_1, and λ_4 are the decay constants of ^{230}Th, ^{231}Pa, and ^{234}U, respectively.

Most reported dates have been measured by the $^{230}Th/^{234}U$ method, which has an effective range of 350,000 years.

Karsologie I: mikroklimatologie jeskyní

Karsologie I: mikroklimatologie jeskyní

Karsologie I: mikroklimatologie jeskyní

Karsologie I: mikroklimatologie jeskyní

Karsologie I: mikroklimatologie jeskyní

Karsologie I: mikroklimatologie jeskyní

Karsologie I: mikroklimatologie jeskyní

Karsologie I: mikroklimatologie jeskyní

Karsologie I: mikroklimatologie jeskyní

Karsologie I: mikroklimatologie jeskyní

Karsologie I: mikroklimatologie jeskyní

Karsologie I: mikroklimatologie jeskyní

Karsologie I: mikroklimatologie jeskyní

Karsologie I: mikroklimatologie jeskyní

Karsologie I: mikroklimatologie jeskyní

Karsologie I: mikroklimatologie jeskyní

Karsologie I: mikroklimatologie jeskyní

Karsologie I: mikroklimatologie jeskyní

Karsologie I: mikroklimatologie jeskyní

BASIC GEOCHRONOLICAL PRINCIPLES AND ASSUMPTIONS

General principles of ^{230}Th-^{234}U-^{238}U and ^{231}Pa-^{235}U dating

Uranium series ***disequilibrium dating methods*** are based on the following radio-nuclide decay chain

$$^{238}\mathrm{U} \xrightarrow[(4.49\times10^{9}\,\mathrm{yr})]{} {}^{234}\mathrm{U} \xrightarrow[(2.48\times10^{5}\,\mathrm{yr})]{} {}^{230}\mathrm{Th} \xrightarrow[(7.5\times10^{4}\,\mathrm{yr})]{} {}^{206}\mathrm{Pb}_{\mathrm{stable}}$$

where the numbers in brackets are half-lives of the decay from one element or isotope to another.

The half life of ^{234}U to ^{230}Th decay is ≈ 10^5 years, and within the age range for dating suitable Pleistocene samples.

In a closed system, the $(^{230}Th/^{238}U)_A$ and $(^{231}Pa/^{235}U)_A$ activity ratios are a function of time (T) and governed respectively by the following equations, assuming an initial state of $^{230}Th = {}^{231}Pa = 0$.

$$\left(\frac{^{230}\mathrm{Th}}{^{238}\mathrm{U}}\right)_{\mathrm{A}} = 1 - e^{-\lambda_{230}T} \qquad \left(\frac{^{231}\mathrm{Pa}}{^{235}\mathrm{U}}\right)_{\mathrm{A}} = 1 - e^{-\lambda_{231}T}$$

If initial $(^{234}U/^{238}U)_A$ in the waters can be reasonably estimated *a priori*, the following relationship can be used to establish the time *T* since deposition,

$$\delta^{234}U(T) = \delta^{234}U(0)e^{-\lambda_{234}T}$$

where $\delta^{234}U = 1000*[(^{234}U/^{238}U)_m / (^{234}U/^{238}U)_{eq} - 1]$,
$(^{234}U/^{238}U)_m$ is the measured mass ratio
$(^{234}U/^{238}U)_{eq}$ is the mass ratio at secular equilibrium.

Reasonable age estimates have been derived for subaqueous speleothem deposits from groundwaters that exhibit minimal long-term variation in $\delta^{234}U(0)$ (Winograd et al. 1988; Ludwig et al. 1992). However, secular variation of $\delta^{234}U(0)$ within individual samples is commonly observed (see Section 2.4), thus limiting the applicability of this technique.

Nearly all natural waters contain ^{234}U and ^{238}U in a state of disequilibrium (i.e., $(^{234}U/^{238}U)_A \neq 1$). Generally $(^{234}U/^{238}U)_A > 1$, and in some cases as high as 30, hence, a second term must be added to Equation (1), which gives the standard $^{230}Th/^{238}U$ age equation

$$\left(\frac{^{230}Th}{^{238}U}\right)_A = 1 - e^{-\lambda_{230}T} + \left(\frac{\delta^{234}U(T)}{1000}\right)\left(\frac{\lambda_{230}}{\lambda_{230} - \lambda_{234}}\right)\left(1 - e^{(\lambda_{234} - \lambda_{230})T}\right)$$

The ^{230}Th age is derived from the following equation

$$1-\left(\frac{^{230}\mathrm{Th}}{^{238}\mathrm{U}}\right)_{act}=e^{-\lambda_{230}T}-\left\{\frac{\delta^{234}\mathrm{U}(0)}{1000}\right\}\left(\frac{\lambda_{230}}{\lambda_{230}-\lambda_{234}}\right)\left(1-e^{(\lambda_{234}-\lambda_{230})T}\right)$$

where T is the age in years, λ represents the decay constant for each nuclide, and (act) refers to activity ratio.

$\lambda_{238} = 1.551\times10^{-10}\ yr^{-1}$

$\lambda_{234} = 2.835\times10^{-6}\ yr^{-1}$

$\lambda_{230} = 9.195\times10^{-6}\ yr^{-1}$

$\delta^{234}U$ is a reformulation of the $^{234}U/^{238}U$ ratio introduced by Edwards *et al*. (1987):

$$\delta^{234}\mathrm{U}(0)=\left[\left\{\left(^{234}\mathrm{U}/^{238}\mathrm{U}\right)/\left(^{234}\mathrm{U}/^{238}\mathrm{U}\right)_{eq}\right\}-1\right]\times10^{3}$$

where, $(^{234}U/^{238}U)_{eq} = \lambda_{238}/\lambda_{230} = 5.472\times10^{-5}$ is the atomic ratio at secular equilibrium.

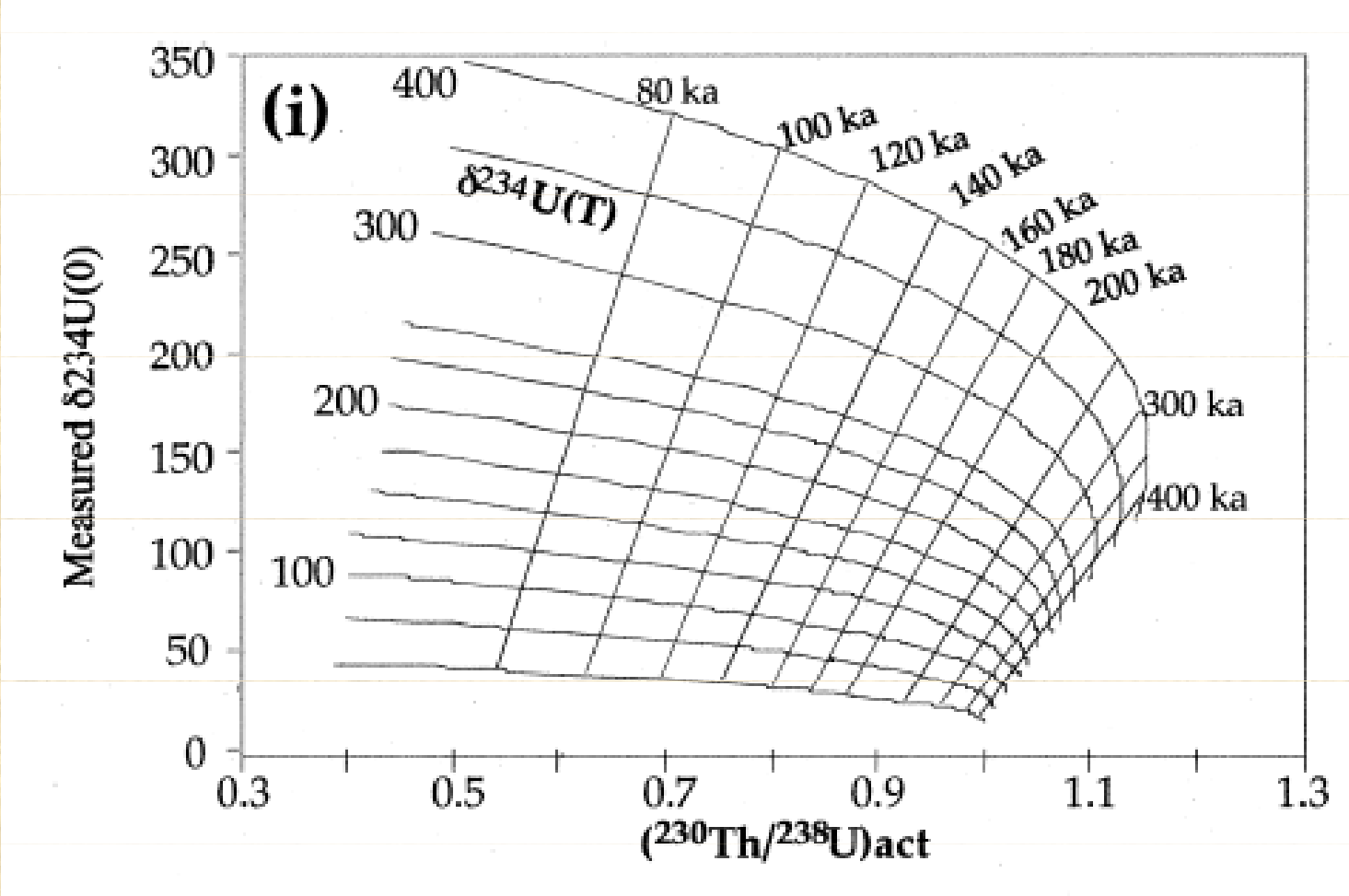

Measured $^{234}U/^{238}U$ plotted as a function of $^{230}Th/^{238}U$ activity ratio. Contours depict variations in $\delta^{234}U(T)$ (horizontal), and age T (vertical lines). Unaltered corals lie along the $\delta^{234}U(T)$ = 150 per mil contour. Open system behavior results in departures from this line in a loose array to older ages and higher values of $\delta^{234}U(T)$.

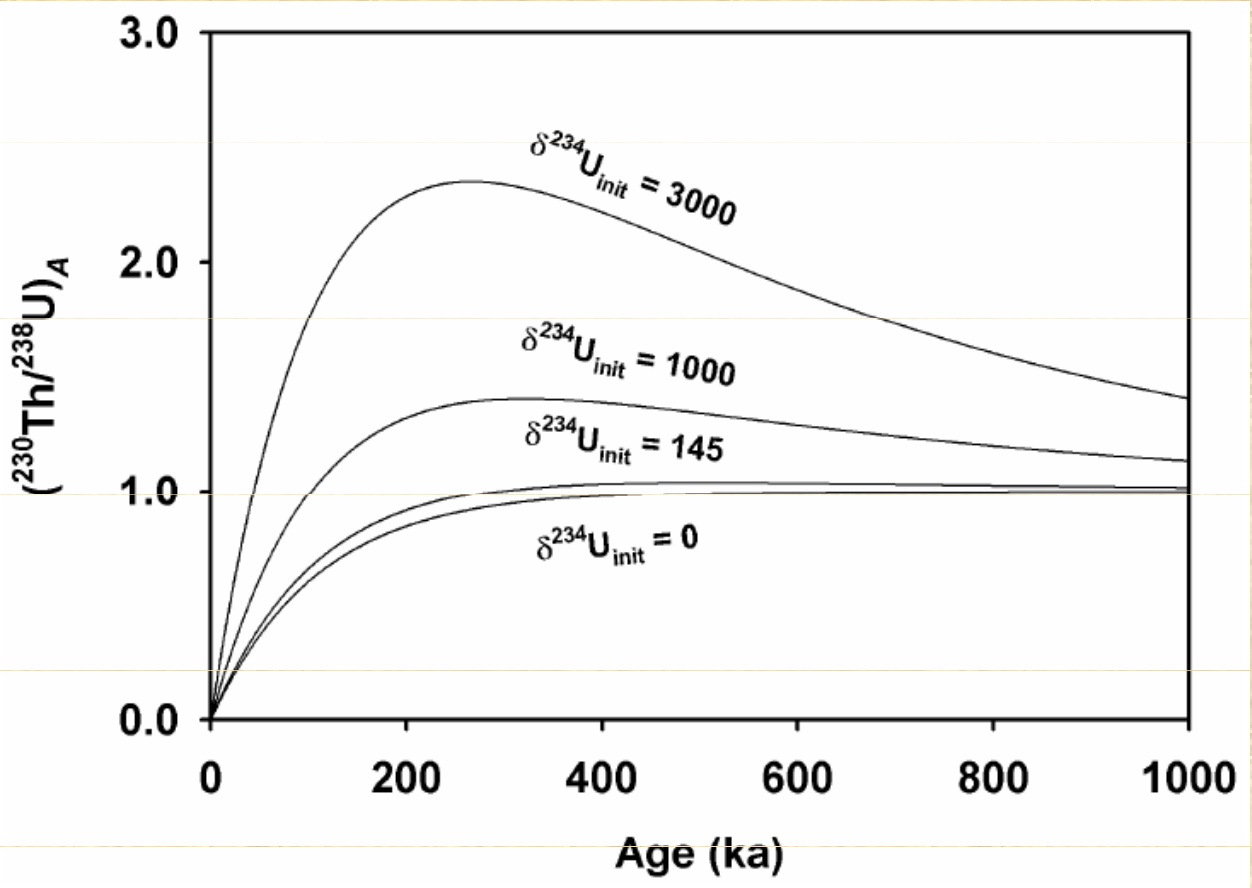

$(^{230}Th/^{238}U)_A$ versus time for different $\delta^{234}U(0)$ values assuming closed system and initial $^{230}Th = 0$ (Eqns. 1 and 2). For those cases where $(^{230}Th/^{238}U)_A > 1$, a unique combination of $(^{230}Th/^{238}U)_A$ and $\delta^{234}U_m$ defines the age *T*. $\delta^{234}U(0)$ >6000 have been observed in speleothems but are generally -100 to 1000.

Figure shows $(^{230}Th/^{238}U)_A$ plotted as a function of *T* for different values of $\delta^{234}U(0)$. As *T* becomes large, $(^{230}Th/^{238}U)_A$ approaches unity and the age limit of the technique is reached. The actual limit depends on the precision of the isotopic determinations and $\delta^{234}U(0)$. Equations (2) and (4) can be combined to give an expression of $^{231}Pa/^{230}Th$

$$\left(\frac{^{231}Pa}{^{230}Th}\right)_A = \frac{\left(\frac{^{235}U}{^{238}U}\right)_A \left(1 - e^{-\lambda_{231}T}\right)}{1 - e^{-\lambda_{230}T} + \left(\frac{\delta^{234}U(T)}{1000}\right)\left(\frac{\lambda_{230}}{\lambda_{230} - \lambda_{234}}\right)\left(1 - e^{(\lambda_{234} - \lambda_{230})T}\right)}$$

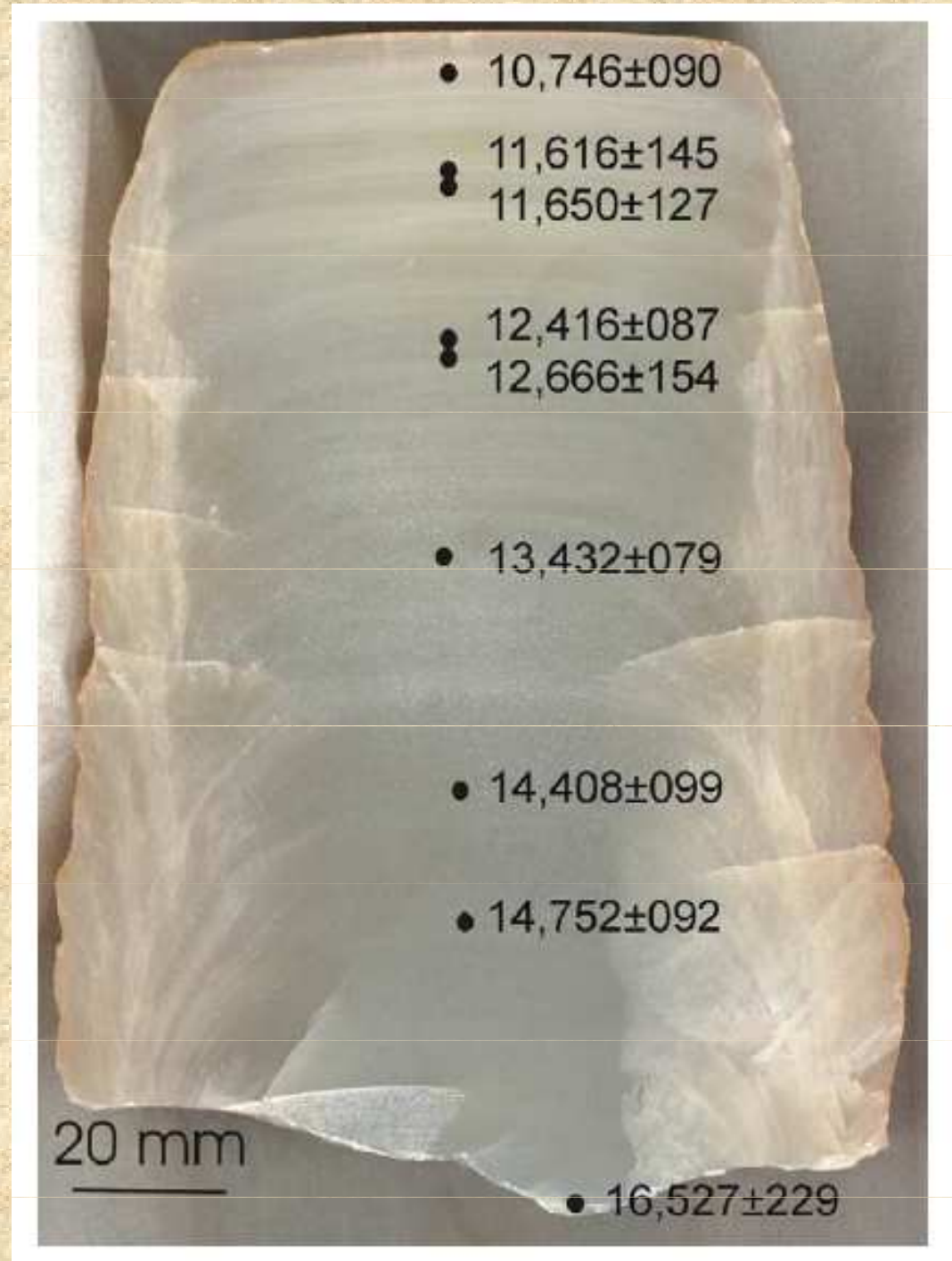

Photograph of the cross-section in stalagmite from Tangshan Cave indicating the ^{230}Th ***ages*** and 2σ errors in yr BP.

Uranium-series data and derived ages of stalagmite T5, Cold Air Cave, Northern Province, South Africa

Depth (mm)	U (ppm)	$^{234}U/^{238}U$	$^{230}Th/^{234}U$	$^{230}Th/^{232}Th$	Age (years)
12 ± 6.5	0.28	9.445 ± 0.271	0.0084 ± 0.0025	3.67	910 ± 280
97 ± 10.5	1.4	8.883 ± 0.096	0.0057 ± 0.0004	>1000	620 ± 40
149 ± 5.5	3.1	8.300 ± 0.093	0.0054 ± 0.0004	>1000	580 ± 50
159 ± 5.0	3.9	7.990 ± 0.107	0.0054 ± 0.0005	>1000	590 ± 50
216 ± 6.0	3.4	8.481 ± 0.094	0.0071 ± 0.0004	>1000	780 ± 40
224 ± 3.0	3.2	8.764 ± 0.191	0.0055 ± 0.0004	>1000	590 ± 50
230 ± 3.0	3	8.104 ± 0.102	0.0076 ± 0.0006	>1000	820 ± 60
235 ± 3.0	3.6	8.195 ± 0.095	0.0064 ± 0.0004	>1000	700 ± 50
242 ± 3.5	1.1	8.197 ± 0.177	0.0073 ± 0.0010	>1000	800 ± 110
258 ± 10.	1.4	8.182 ± 0.144	0.0369 ± 0.0019	>1000	4060 ± 220
275 ± 5.5	1.5	8.091 ± 0.105	0.0396 ± 0.0013	>1000	4360 ± 150
288 ± 7.5	1.4	7.780 ± 0.100	0.0397 ± 0.0018	>1000	4380 ± 200

New ^{230}Th dates determined for D3 stalagmites. All ages were corrected for initial ^{230}Th using the value $(7\pm5)\times10^{-6}$, a value calculated from the initial $^{230}Th/^{232}Th$ ratios required to place several samples with anomalously high ^{232}Th values in correct stratigraphic order (Yuan et al., 2004; Dykoski et al., 2005).

Table 1
^{230}Th dating results for stalagmites D3 and D4 by ICP-MS analysis

Sample number	Depth (cm)	^{238}U (ppb)	^{232}Th (ppt) [a]	$\delta^{234}U$ (measured)	$^{230}Th/^{238}U$ (activity)	^{230}Th age (ka; uncorrected)	^{230}Th age (ka; corrected)	$\delta^{234}U_{Initial}$ (corrected)	Growth rate [b] (μm/year)
D3									
D3F1	35.0	648±1.0	3865±47	−212.5±1.4	0.4560±0.0019	100.2±0.8	99.7±0.8	−281.8±2.0	
D3F2	47.3	657±1.0	260±32	−225.4±1.4	0.4484±0.0017	100.6±0.7	100.6±0.7	−299.4±1.9	153
D3E1	62.1	797±1.4	4549±44	−192.3±1.3	0.4844±0.0021	105.7±0.9	105.3±0.9	−259.3±1.9	31
D3D1	78.7	804±2.3	352±40	−187.3±1.6	0.5028±0.0021	111.6±1.0	111.6±1.0	−256.8±2.3	27
D3D4a [c]	93.3	1098±2.1	610±45	−190.0±1.4	0.5041±0.0019	112.9±0.9	112.9±0.9	−261.4±2.0	85
D3D4b [c]	93.3	1091±2.0	597±40	−190.1±1.4	0.5058±0.0019	113.7±0.9	113.6±0.9	−262.2±2.0	–
D3D5	103.4	784±1.3	159±44	−195.2±1.4	0.5038±0.0020	114.4±0.9	114.4±0.9	−269.7±2.0	88
D3D2a [c,d]	109.4	1124±2.2	420±46	−200.1±1.8	0.5061±0.0022	117.0±1.1	117.0±1.1	−278.4±2.7	22
D3D2b [c,d]	109.4	1129±3.8	570±61	−201.8±2.6	0.5070±0.0024	118.0±1.4	118.0±1.4	−281.6±3.8	–
D3D3 [d]	111.1	944±1.7	231±41	−208.7±1.5	0.4999±0.0019	117.2±1.0	117.2±1.0	−290.6±2.2	–
D3C1N	122.3	1279±2.2	563±41	−196.0±1.2	0.5134±0.0020	118.9±1.0	118.9±1.0	−274.2±1.9	82
D3B2	139.8	1101±1.9	524±48	−206.5±1.3	0.5090±0.0020	120.6±1.0	120.5±1.0	−290.3±2.0	104
D3B3a [c,d]	148.5	1006±1.9	1760±47	−194.1±1.3	0.5219±0.0021	122.1±1.1	121.9±1.1	−274.1±2.1	59
D3B3b [c,d]	148.5	1003±1.9	2059±48	−195.0±1.4	0.5240±0.0024	123.4±1.2	123.2±1.3	−276.3±2.2	–
D3B1 [d]	156.3	534±0.9	4139±52	−190.9±1.3	0.5256±0.0019	122.6±1.0	122.1±1.0	−269.7±2.0	–
D3A2	161.0	1016±2.0	466±41	−198.4±1.5	0.5234±0.0020	124.4±1.1	124.3±1.1	−282.0±2.4	52
D3A1	177.7	954±1.8	1887±43	−192.8±1.5	0.5301±0.0023	125.4±1.2	125.3±1.2	−274.8±2.3	170

ppt=parts per trillion.

Decay constant values are $\lambda_{230}=9.1577\times10^{-6}$ year^{-1}, $\lambda_{234}=2.8263\times10^{-6}$ year^{-1}, $\lambda_{238}=1.55125\times10^{-10}$ year^{-1}. Corrected ^{230}Th ages assume the initial $^{230}Th/^{232}Th$ atomic ratio of $(7\pm5)\times10^{-6}$.

Table 1
Mass spectrometric U–Th ages for stalagmite 996182 from Tangshan Cave

Sample name	Distance from top (mm)	U (ppm)	^{232}Th (ppb)	(^{230}Th/^{232}Th)	(^{234}U/^{238}U)	(^{230}Th/^{238}U)	^{230}Th age (yr BP)	Initial (^{234}U/^{238}U)
WYJ-5	5.0 ± 1.5	0.1194	0.273	155	1.2384 ± 31	0.1169 ± 09	10 746 ± 090	1.2458 ± 32
WYJ-17.5	17.5 ± 1.0	0.1555	0.015	3890	1.2176 ± 32	0.1237 ± 14	11 616 ± 145	1.2249 ± 33
WYJ-20.5	20.5 ± 1.0	0.1541	0.013	4439	1.2113 ± 33	0.1234 ± 12	11 650 ± 127	1.2184 ± 33
WYJ-41.5	41.5 ± 1.5	0.1568	0.010	6142	1.1922 ± 31	0.1291 ± 15	12 425 ± 160	1.1991 ± 32
Replicate		0.1626	0.008	8385	1.1945 ± 26	0.1292 ± 10	12 412 ± 104	1.2014 ± 27
WYJ-45	45.0 ± 1.0	0.1522	0.011	5549	1.1983 ± 38	0.1321 ± 15	12 666 ± 154	1.2056 ± 39
WYJ-73	73.0 ± 1.5	0.1790	0.020	3816	1.2062 ± 32	0.1405 ± 09	13 424 ± 096	1.2142 ± 33
Replicate		0.1708	0.015	4872	1.2088 ± 24	0.1411 ± 13	13 448 ± 138	1.2169 ± 25
WYJ-106.5	106.5 ± 2.0	0.1108	0.015	3388	1.2088 ± 36	0.1511 ± 14	14 469 ± 154	1.2176 ± 37
Replicate		0.1179	0.009	5694	1.2057 ± 42	0.1497 ± 11	14 366 ± 129	1.2143 ± 44
WYJ-126.5	126.5 ± 2.0	0.1456	0.007	9732	1.2101 ± 38	0.1542 ± 29	14 766 ± 304	1.2191 ± 39
Replicate		0.1400	0.008	7922	1.2038 ± 27	0.1532 ± 09	14 751 ± 096	1.2125 ± 28
WRJ-166	166.0 ± 1.5	0.2258	0.014	8055	1.2003 ± 39	0.1699 ± 21	16 527 ± 229	1.2099 ± 41

The ages are calculated using half-lives from ^{230}Th and ^{234}U of 75 380 and 244 600 yr, respectively. Errors are at 2σ level. U-series isotopic analysis was carried out on the VG Sector 54 thermal ionization mass spectrometer at University of Queensland and detailed analytical procedures were described in [15]. About 0.5 g material was used for each analysis. The age for WYJ-5 includes a small correction for detrital thorium assuming average crustal Th/U = 3.8 ± 1.9 and ^{238}U, ^{234}U, and ^{230}Th are in secular equilibrium. Ages for the other samples are not corrected for detrital thorium because their ^{230}Th/^{232}Th are all higher than 1000 and the correction is negligible. Four samples are analyzed in duplicate, which are all within analytical errors of each other, respectively.

Table 1
Th/U ages.

Lab. No.	Distance from top	$\delta^{234}U$		Conc. ^{238}U		Conc. ^{232}Th		Conc. ^{230}Th		Age	
	(cm)	(‰)	±(‰)	(μg/g)	±(μg/g)	(ng/g)	±(ng/g)	(pg/g)	±(pg/g)	(kyr)	±(kyr)
2080	0.5	23.8	3.7	9.467	0.019	155.48	0.84	56.44	0.42	47.48	0.51
2702	1.7	14.3	2.5	18.169	0.027	3.096	0.022	109.07	0.87	48.95	0.52
2131	3.0	21.7	3.2	28.582	0.057	5.738	0.026	177	1.1	50.44	0.45
2503	6.0	17.1	1.7	34.973	0.035	6.704	0.016	217.04	0.76	50.87	0.26
2569	6.5	14.4	2.1	36.195	0.040	3.866	0.010	224.41	0.67	50.99	0.24
2703	9.4	14.7	1.4	41.682	0.042	2.5778	0.0059	261.5	0.65	51.74	0.20
2504	12.0	11.0	3.1	46.083	0.074	1.589	0.011	290.4	2.3	52.30	0.57
2704	14.4	11.2	1.6	58.948	0.065	8.12	0.019	379.4	1.1	53.71	0.24
2292	16.0	9.3	1.7	41.687	0.050	2.0735	0.0093	269.2	1.1	54.11	0.32
2506	16.0	11.2	1.9	39.787	0.056	4.253	0.015	256	1.5	53.70	0.44
2505	17.0	5.4	1.9	56.311	0.062	1.278	0.010	365.2	3.7	54.70	0.72
2705	20.0	10.4	1.4	74.954	0.075	2.7099	0.0054	490.5	1.0	54.96	0.18
2290	23.0	10.0	2.1	61.349	0.092	0.7281	0.0033	404.3	1.8	55.49	0.38
2507	26.0	8.0	1.9	56.098	0.067	2.964	0.011	373.9	1.9	56.48	0.42
1911	29.0	10.5	3.4	40.398	0.097	2.311	0.012	273.3	1.6	57.38	0.54

Errors are quoted as 2-σ standard deviations.

Table 1
TIMS U–Th results and age estimates for stalagmite Cla4 of Clamouse Cave

	U (ppm)	$^{230}Th/^{232}Th$ (activity)	$^{230}Th/^{234}U$ (activity)	Age (ka)	$+2\sigma$	-2σ	$(^{234}U/^{238}U)_0$ (activity)
Cla4-0.25	0.125	6167	0.5303 ± 0.0025	**74.540**	0.344	0.343	3.7146 ± 0.0069
Cla4-6.7	0.102	7615	0.5356 ± 0.0021	**75.539**	0.296	0.296	3.7024 ± 0.0054
Cla4-8	0.110	7099	0.5713 ± 0.0024	**82.388**	0.343	0.343	3.7728 ± 0.0071
Cla4-26.3	0.121	27669	0.5766 ± 0.0021	**83.326**	0.305	0.305	3.9000 ± 0.0057
Cla4-27.5	0.076	2655	0.6539 ± 0.0034	**99.235**	0.572	0.570	4.2375 ± 0.0078
Cla4-30.3	0.063	404	0.6588 ± 0.0022	**100.299**	0.355	0.354	4.2689 ± 0.0052
Cla4-31.3	0.087	3433	0.6812 ± 0.0031	**105.382**	0.511	0.510	4.2783 ± 0.0081
Cla4-32.8	0.125	1582	0.7267 ± 0.0032	**116.500**	0.581	0.579	4.2186 ± 0.0074
Cla4-33.8	0.075	1914	0.7518 ± 0.0028	**121.624**	0.516	0.515	5.1331 ± 0.0076
Cla4-35.3	0.073	16033	0.7722 ± 0.0027	**125.118**	0.511	0.510	6.9913 ± 0.0099
Cla4-44.4	0.071	7165	0.7833 ± 0.0021	**127.888**	0.399	0.399	7.1554 ± 0.0084
Cla4-45.6	0.078	8393	0.8962 ± 0.0035	**162.884**	0.862	0.859	6.2220 ± 0.0118
Cla4-51.7	0.074	7196	0.9081 ± 0.0052	**168.553**	1.326	1.321	5.5473 ± 0.0151
Cla4-52.5	0.063	677	0.9483 ± 0.0074	**188.211**	2.554	2.507	4.5274 ± 0.0239
Cla4-60.5	0.111	776	0.9430 ± 0.0160	**186.517**	7.480	7.020	4.4049 ± 0.0676

The names of the samples represent the name of the stalagmite (Cla4) and the location of the sample center in cm from the top. The age is the apparent $^{230}Th/^{234}U$ age, all errors are calculated by error propagation and given at the 2σ level. $^{230}Th/^{234}U$ ratios are activity ratios relative to HU1 assumed to be at secular equilibrium. Repeated analysis ($n = 10$) of HU1 uraninite standard yields a mean $^{234}U/^{238}U$ activity ratio of 1.0026 with a reproducibility (2 S.D.) of 0.0050 and a mean $^{230}Th/^{234}U$ activity ratio of 1.0015 with a reproducibility of 0.0066. Decay constants used: $\lambda^{230}Th = 9.1953 \times 10^{-6}$, $\lambda^{234}U = 2.8338 \times 10^{-6}$, $\lambda^{238}U = 1.55125 \times 10^{-10}$.

Table 1
Uranium and thorium isotopic ratios and $^{230}Th/^{234}U$ ages

Sample	Distance from bottom[a] (mm)	^{238}U (ng/g)	^{232}Th (pg/g)	$\delta^{234}U$[b,c] measured	$^{230}Th/^{238}U$ activity	$^{230}Th/^{232}Th$ atomic	Uncorrected age (yr)	Corrected age[d] (yr)
ON-3-B	19	266	9740	1599 (7)	1.18E-2 (0.6)	1.39E-4 (1)	13580 (180)	13110 (260)
ON-3-B-a	48	283	9480	1870 (7)	3.35E-1 (3)	1.65E-4 (2)	13400 (130)	13070 (210)
ON-3-B-b	48	282	7920	1870 (8)	3.33E-1 (3)	1.96E-4 (2)	13310 (140)	13030 (190)
ON-3-B	75	268	4840	1826 (8)	3.15E-1 (4)	2.86E-4 (4)	12730 (160)	12510 (190)

ON-3-B-a and ON-3-B-b are replicate samples analyzed from a homogenized powder drilled from a single area of the speleothem.

[a] The total length of ON-3-B is 16.5 cm.

[b] $\delta^{234}U_{measured} = [(^{234}U/^{238}U)_{measured}/(^{234}U/^{238}U)_{eq} - 1] \times 10^3$, where $(^{234}U/^{238}U)_{eq}$ is the secular equilibrium atomic ratio: $\lambda_{238}/\lambda_{234} = 5.472 \times 10^{-5}$.

[c] Values in parentheses represent 2σ errors in the last significant figure.

[d] Unsupported ^{230}Th was corrected using an initial $^{230}Th/^{232}Th$ ratio of 4.4×10^{-6} ($\pm 2.2 \times 10^{-6}$) representative of average crustal silicates.

Table 2
Uranium series TIMS data and age estimates for the stalagmite ST-JA3

Sample	Distance from top (mm)	^{238}U (μg/g)	$^{234}U/^{238}U$	Age (yr BP)	$^{230}Th/^{232}Th$	Corrected age
7	215	1.9163±0.0126	1.0579±0.0168	1822±23	112	1802±23
10	312	2.1044±0.0055	1.0546±0.0064	2675±26	>500	2665±26
11	337	2.0532±0.0031	1.0559±0.0035	2942±32	446	2932±32
13	409	2.0429±0.0083	1.0439±0.0114	3476±39	>500	3466±39

Table 1
U–Th isotopic data for stalagmite LYN from Lynds Cave, Tasmania, Australia

Sample Name	Distance from top (mm)	U (ppm)	^{232}Th (ppb)	^{230}Th/^{232}Th	^{234}U/^{238}U	^{230}Th/^{238}U	Uncorrected ^{230}Th Age (yr BP)	Corrected ^{230}Th Age (yr BP)	Initial ^{234}U/^{238}U
LYN-T	9	0.0407	0.073	124.1	1.5927 ± 80	0.0731 ± 07	5094 ± 59	5061 ± 74	1.6016 ± 83
LYN-1	110	0.0613	0.216	89.5	1.9942 ± 56	0.1039 ± 15	5792 ± 89	5741 ± 112	2.0114 ± 63
LYN-2b	202	0.0597	0.102	212.9	2.0208 ± 71	0.1194 ± 17	6593 ± 97	6568 ± 108	2.0405 ± 75
LYN-2	206	0.0626	0.096	238.1	2.0129 ± 49	0.1200 ± 57	6653 ± 325	6631 ± 334	2.0325 ± 53
LYN-3	347	0.0486	0.110	151.0	1.7723 ± 47	0.1126 ± 08	7105 ± 56	7068 ± 73	1.7884 ± 50
LYN-4	479	0.1018	1.575	23.7	1.8223 ± 74	0.1209 ± 11	7428 ± 78	7179 ± 188	1.8428 ± 99
LYN-5	566	0.0871	0.448	69.7	1.7683 ± 41	0.1180 ± 20	7474 ± 130	7389 ± 169	1.7857 ± 49
LYN-6b	642	0.0758	0.428	78.1	2.0908 ± 57	0.1453 ± 13	7788 ± 77	7709 ± 111	2.1166 ± 69
LYN-6b-r	642	0.0715	0.338	94.8	2.1069 ± 85	0.1475 ± 18	7844 ± 106	7779 ± 134	2.1330 ± 96
LYN-6	650	0.0925	0.424	103.3	2.2104 ± 34	0.1562 ± 55	7922 ± 289	7861 ± 315	2.2392 ± 46
LYN-7	777	0.0835	0.482	69.3	1.8026 ± 49	0.1318 ± 22	8211 ± 143	8117 ± 185	1.8225 ± 58
LYN-8	926	0.0668	1.250	21.8	1.7088 ± 75	0.1347 ± 13	8881 ± 99	8560 ± 239	1.7299 ± 101
LYN-B2	1094	0.0920	0.844	60.0	2.2168 ± 77	0.1814 ± 31	9218 ± 166	9097 ± 216	2.2517 ± 99
LYN-B	1119	0.0721	3.209	12.5	2.1107 ± 35	0.1832 ± 52	9798 ± 290	9181 ± 548	2.1540 ± 130

Isotopic ratios refer to activity ratios. All errors are quoted at 2σ level and in the last two significant figures. ^{230}Th ages are calculated using program ISOPLOT/EX [49] and half-lives from ^{230}Th and ^{234}U of 75 380 and 244 600 yr, respectively. The corrected ^{230}Th ages and initial (^{234}U/^{238}U) ratios include a small correction for initial/detrital U and Th using average crustal ^{232}Th/^{238}U atomic ratio of 3.8 ± 1.9 (^{230}Th, ^{234}U and ^{238}U are assumed to be in secular equilibrium)[25]. LYN-6b-r is a replicate analysis of LYN-6b (separate speleothem chips of the same sample).

All isotopes of interest (^{229}Th, ^{230}Th, ^{232}Th, ^{233}U, ^{234}U, ^{235}U, ^{236}U) were measured on an ion-counting Daly multiplier with abundance sensitivity in the range of 20 ppb

Thermal ionization mass spectrometric (TIMS) $^{230}Th/^{234}U$ dating has been carried out on intercalated speleothem samples from the limestone cave occupied by *Homo erectus* at Zhoukoudian, China.

Table 1 TIMS U-Series analyses on speleothem samples from Locality 1, Zhoukoudian

Sample	^{238}U (ppb)	$^{230}Th/^{232}Th$	$^{234}U/^{238}U$	$^{230}Th/^{234}U$	^{230}Th age (ka)
			Samples from Layers 1–2, Locus H		
95-4	1368 (2)	294 (2)	1.2008 (0.0015)	0.7552 (0.0026)	144 (1)
89-3 (top)	410.5 (0.6)	281 (2)	1.1354 (0.0018)	0.9927 (0.0037)	337 (8)
95-3	427.0 (0.9)	55.7 (0.7)	1.2086 (0.0029)	0.9855 (0.0045)	298 (7)
89-3 (I)	82.2 (0.1)	233 (2)	1.1421 (0.0025)	1.0162 (0.0045)	391 $(^{+16}_{-15})$
(II)	75.5 (0.1)	289 (4)	1.1399 (0.0028)	1.0162 (0.0094)	393 $(^{+35}_{-28})$
(III)	77.0 (0.1)	1550 (9)	1.1393 (0.0020)	1.0197 (0.0076)	406 $(^{+33}_{-26})$
(IV)	71.73 (0.04)	650 (5)	1.1449 (0.0016)	1.0197 (0.0030)	400 $(^{+12}_{-11})$

Holocene speleothems: examples from a cave system in Rana, northern Norway

Table 1
TIMS U-series dating results from sample SG95

Lab no.	mm from base	^{238}U conc. (ppm)	^{232}Th conc. (ppm)	$^{234}U/^{238}U$	$^{230}Th/^{234}U$	$^{230}Th/^{232}Th$	$^{234}U/^{232}Th$	Age (years before AD2000)	Age (years AD/BC)
197	30–35	1.1055 ± 0.0005	0.389	1.7142 ± 0.0021	0.0351 ± 0.0003	23.1 ± 0.3	658 ± 9	3875 ± 34	1875 ± 34BC
198	39–44	1.2754 ± 0.0006	0.327	1.7156 ± 0.0020	0.0321 ± 0.0002	29.0 ± 0.3	905 ± 9	3538 ± 17	1538 ± 17BC
214	50–55	1.2589 ± 0.0005	1.365	1.7057 ± 0.0019	0.0290 ± 0.0002	11.7 ± 0.1	404 ± 4	3201 ± 19	1201 ± 19BC
215	65–70	1.0586 ± 0.0010	0.226	1.7012 ± 0.0041	0.0258 ± 0.0002	52.0 ± 0.5	2019 ± 24	2835 ± 20	835 ± 20BC
200	75–80	1.0836 ± 0.0004	0.150	1.6955 ± 0.0019	0.0228 ± 0.0002	38.2 ± 0.4	1680 ± 20	2501 ± 17	501 ± 17BC
201	90–95	0.9246 ± 0.0005	0.288	1.6991 ± 0.0020	0.0196 ± 0.0001	14.6 ± 0.2	745 ± 10	2148 ± 15	148 ± 15BC
209	115–120	1.0567 ± 0.0005	0.852	1.7098 ± 0.0019	0.0156 ± 0.0001	8.6 ± 0.1	553 ± 6	1712 ± 7	AD288 ± 7
216	128–133	0.6254 ± 0.0003	0.227	1.7192 ± 0.0023	0.0090 ± 0.0001	10.9 ± 0.1	1201 ± 15	989 ± 7	AD1011 ± 7
202	137–142	0.8686 ± 0.0004	0.074	1.7414 ± 0.0022	0.00575 ± 0.00004	15.8 ± 0.2	2751 ± 39	629 ± 5	AD1371 ± 5
210	155–159	1.1132 ± 0.0005	0.102	1.7142 ± 0.0021	0.00270 ± 0.00003	13.2 ± 0.2	4876 ± 80	296 ± 3	AD1704 ± 3

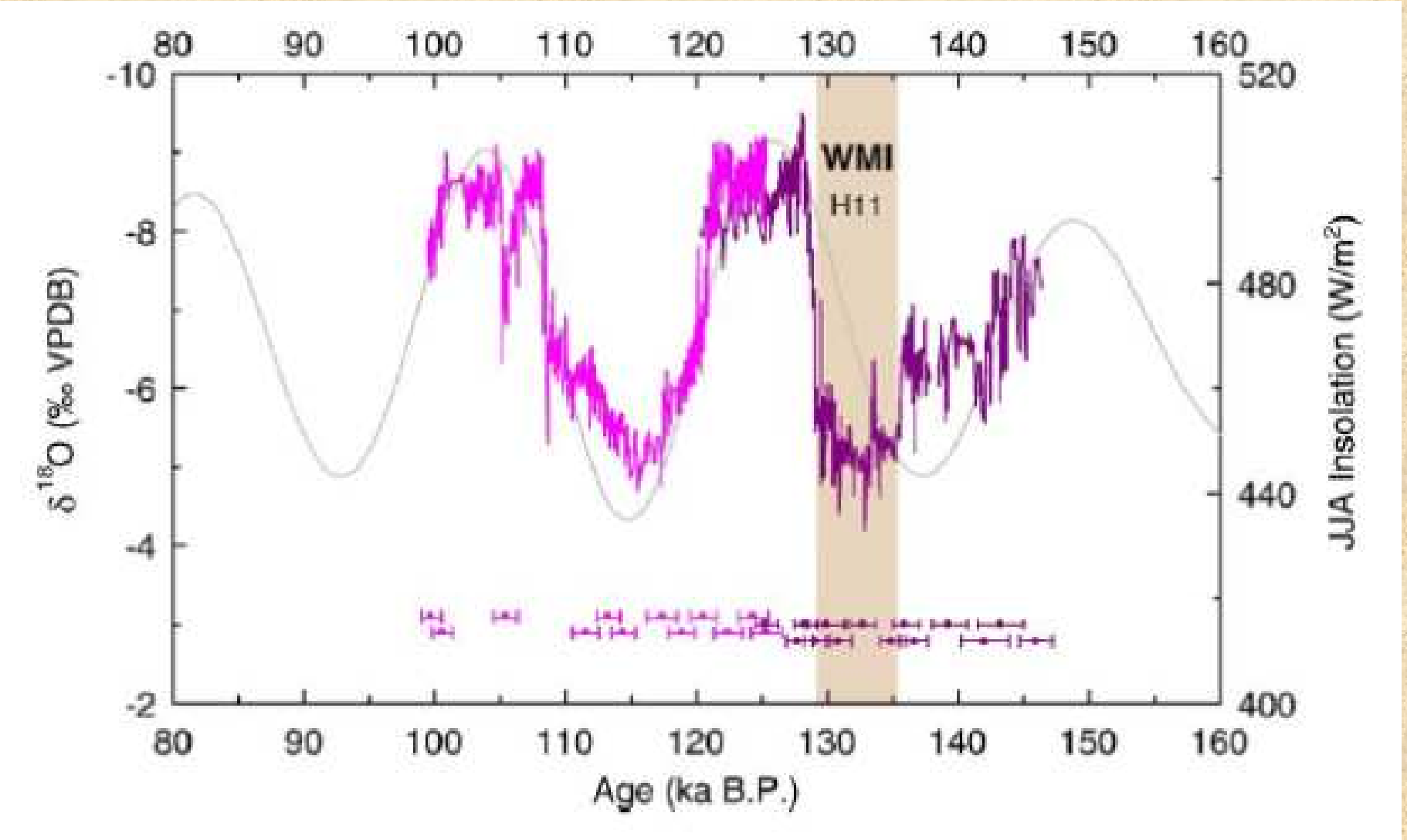

New δ18O time series for speleothems D3 (pink), D4 (purple), and summer insolation at 25°N (dashed line) integrated over the months of June, July, and August (Berger, 1978).

V přírodě je uran v nízkých koncentracích 0,04 – 3 %. Vyskytuje se zde jako směs izotopů – ^{238}U (99,276 %), ^{235}U (0,718 %), ^{234}U (0,004 %).

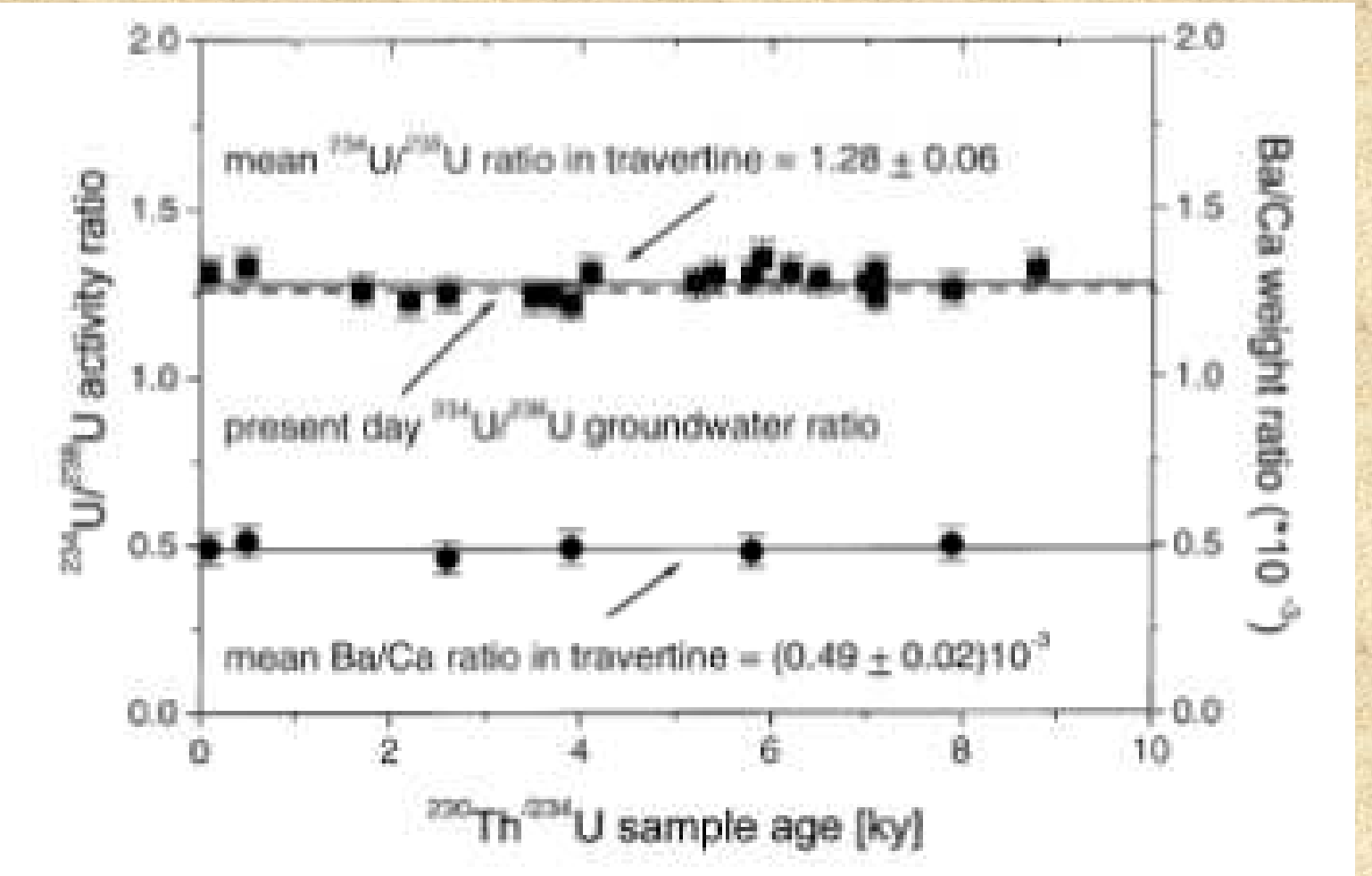

Relativní poměr $^{234}U/^{238}U$ v horninách 1.28+0.06 nezávislý na čase.

Dnešní poměr $^{234}U/^{238}U$ podzemních vod (1.27±0.04)? V nerovnováze $(^{234}U/^{238}U)_A \neq 1$). Obecně $(^{234}U/^{238}U)_A > 1$, v některých případech až 30.